

Advanced Dynamics MDOF

Modal Analysis Report

Authors:

Sofia Bertocci - 3761479
Oriol Jo López - 3759431
Rowan Lawlor - 3150135

Advanced Dynamics

Supervisors: Dario Di Maio

Contents

1.	Introduction.....	5
1.1.	Materials & Machines	5
1.2.	System Set-up.....	6
2.	Theoretical Description.....	7
2.1.	Geometrical characterization of the system.....	7
2.2.	Stiffness characterization	8
2.3.	Single-DOF Platform System.....	9
2.4.	Multiple-DOF Platform Cylinder System.....	10
3.	Modal Test & Analysis.....	12
3.1	Procedure.....	12
3.2	SDOF Results & Analysis	13
3.3	MDOF Results & Analysis.....	16
4.	Discussion	19
5.	Conclusion.....	20
	Appendix A – Component Dimensions & Mass	21
	Appendix B – Theoretical Calculation	22
	Appendix C – Line Fit Method Analysis Functions	26
	Appendix D – All Analysis Graphs	28
1.	SDOF 1-1	28
2.	SDOF 2-2	32
2.	MDOF 1-1	36
3.	MDOF 1-2	41

1. Introduction

It is quite common for an engineer to interface with systems, both Single-DOF and Multiple-DOF, that present oscillations and vibrations. It is therefore essential to know how to analyze them, in order to design secure solutions for the real world.

The advanced dynamics module ended with a laboratory experience, in which percussion was practiced on a scale model, to analyze the related vibrations. In this report the experience and the analysis carried out will be described, underlining the theoretical model that is behind it.

This report will first introduce the system and its components, along with the procedure which will be followed. Then, a theoretical model of the system and its frequencies will be made, to act as an ‘expected’ outcome of the experiment. Following that the results of the experiment will be introduced and analyzed for the observed frequencies. Finally, the results of the theoretical and experimental analysis will be discussed. This report should give an idea of how well the theoretical and experimental model of an MDOF system compare.

1.1. Materials & Machines

To perform this experiment a number of materials were required, these were:

Material	Quantity
<i>MDOF System</i>	
Part 1 – Wood block on aluminum frame	1
Part 2 – Cylinder bounded by elastic band	1
<i>Testing Equipment</i>	
5 kN Modal Hammer	1
Accelerometer	1
Digital-Analog-Converter	1
Desktop Computer	1
<i>Miscellaneous</i>	
Ruler	1

1.2. System Set-up

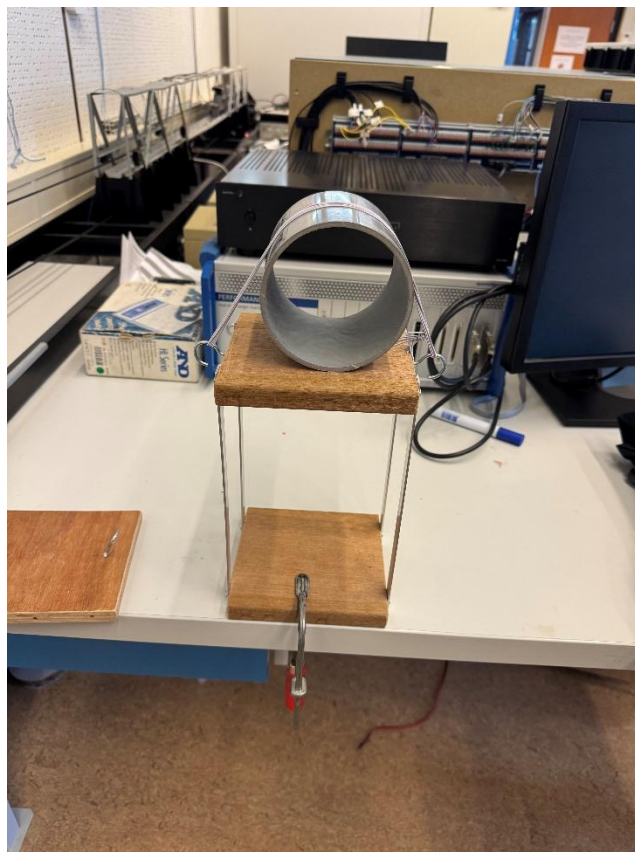


Figure 1: The full MDOF system, as seen in the laboratory.

As can be seen above, the full system is composed of the following two components:

- Part 1 is a wooden block sitting on four thin aluminum supports with a hook on either side.
- Part 2 is a plastic cylinder which is bounded on top to a wooden block below by two hooks on its side.

The physical properties, such as dimensions and mass, can be seen in Appendix A.

Those parts each comprise a single degree-of-freedom system. From this, Part 2's cylinder is then placed on Part 1, taking over the role of its base block. This now creates the full multiple degree-of-freedom system which can be seen above. This system will be the subject of this experiment.

2. Theoretical Description

The aim of this section is to model and characterize the dynamic behavior of both single-degree-of-freedom (SDOF) and the multiple-degree-of-freedom (MDOF) mechanical systems which have been explained before. The study proceeds in two stages.

First, the platform and frame are analyzed as a SDOF system in lateral translation. Second, the coupled platform–cylinder configuration is modeled as a two-degree-of-freedom (2DOF) system, where the platform can translate, and the cylinder can rotate.

For each case, we:

1. Measure the relevant physical properties of the system
2. Determine equivalent stiffnesses
3. Derive the undamped equations of motion
4. Compute the undamped natural frequencies

The final goal is to obtain a predictive model to compare it with experimental modal data.

Along the way, several simplifying assumptions are made (rigid bodies, ideal springs, linear behavior). These assumptions introduce uncertainty, which will be discussed explicitly. The full derivations of the equations of motion and the MATLAB script used to compute the natural frequencies are provided in Appendix A and B and will be referenced throughout this report.

2.1. Geometrical Characterization of the System

To compute the undamped equations of motion of the system as well as the undamped natural frequencies it had to be geometrically characterized.

The weight and dimensions of the different parts of both systems were needed to complete the equations. The procedure to get those values was the following:

- Aluminum Beams

By calculating the volume of each beam, using the values from Appendix A, and with the density of aluminum, a rough estimation was made for the weight of the 4 beams.

$$m_b = 0.072 \text{ kg}$$

- Platform

Using a scale from the laboratory, the total weight of the frame (top and bottom platforms, 4 aluminum beams, two hooks and some bolts) was weighed. The weight of the aluminum beams was subtracted, and the result was divided by two.

$$m_p = 0.303 \text{ kg}$$

- Cylinder

The value of the cylinder's weight was directly obtained from the scale, and it is in Appendix A.

$$m_c = 0.129 \text{ kg}$$

All the measurements were measured with a ruler with a precision of 1 mm and these values can be found on Appendix A. The calculations needed to get the mass values from this section can be found in Appendix B.

2.2. Stiffness characterization

To predict vibration behavior, we need equivalent stiffness values for:

1. The frame in lateral translation (k_x)
2. The elastic cord restraining the cylinder (k_θ)

For frame stiffness, it was only considered the stiffness of the beams. Since the force that we apply to the SDOF has the same direction as the axe x, the platform stiffness has been entitled as k_x and its value is 3707.760 N/m. The calculations are on Appendix B.

On the other hand, the stiffness of the spring (k_s) had to be calculated. Once the value was obtained, it was converted to torsional stiffness; the cylinder in the MDOF system rotates, instead of sliding, so the spring produces a torque to the cylinder (k_θ). The values of these stiffnesses are 73.09 N/m and 0.221 N/m respectively, the calculation of these can be found on Appendix B.

The following figure shows the frame setup.

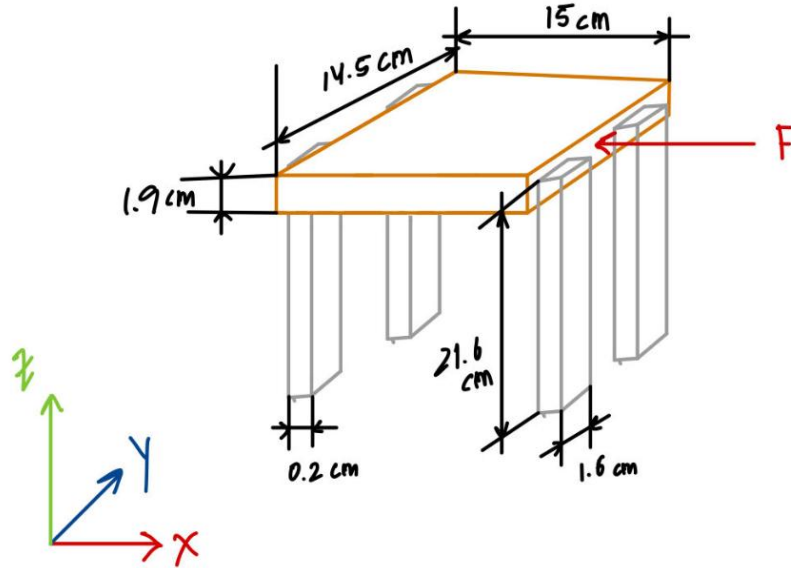


Figure 2: Setup and dimensions of the frame.

2.3. Single-DOF Platform System

Before adding the cylinder, we treat the platform + frame as a single lateral DOF. We assume:

- The platform translates laterally as a rigid body with displacement $x(t)$.
- The four legs bend but remain elastic.
- No rotation of the platform is considered in this simplified model.
- Damping and external forcing are neglected for the natural frequency calculation.

Under those assumptions, the undamped equation of motion is.

$$m_p \ddot{x}(t) + k_x x(t) = 0 \quad (1)$$

$$0.303 \ddot{x}(t) + 3707.760x(t) = 0 \quad (2)$$

Then the undamped natural angular frequency is

$$w_n = \sqrt{\frac{k_x}{m_p}} \quad ; \quad f_n = \frac{w_n}{2\pi} \quad (3) ; (4)$$

The value of the natural frequency is 17.61 Hz.

All intermediate algebra and numeric substitution (mass value, stiffness value, and final frequency in Hz) will be documented in Appendix B.

2.4. Multiple-DOF Platform Cylinder System

To capture the coupled dynamics of the assembled test rig, we extend the model to two generalized coordinates:

- $x(t)$: lateral translation of the platform.
- $\theta(t)$: rotation of the cylinder about its center.

We assume:

1. The cylinder rolls/rocks against the platform without significant slip, so the center of the cylinder moves laterally with the platform.
2. The cylinder's lateral restraint is dominated by the elastic cord, modeled as a torsional spring with stiffness k_θ .
3. The frame is linear and provides a lateral spring of stiffness k_x
4. Damping and external forcing are neglected for the free-vibration model.

With those assumptions, the kinetic energy (KE) of the system includes translational KE of the platform mass, translational KE of the cylinder's center of mass (which is influenced by both x and θ) and rotational KE of the cylinder (through its inertia J).

From that energy description (full derivation in Appendix B), the mass matrix M is:

$$M = \begin{bmatrix} m_p + m_c & m_c r \\ m_c r & m_c r^2 + J \end{bmatrix} = \begin{bmatrix} 0.432 & 0.00710 \\ 0.00710 & 0.00078045 \end{bmatrix} \quad (5)$$

The potential energy comes from the frame acting like a translational spring on x and the cord acting like a torsional spring on θ . This gives the stiffness matrix K as:

$$K = \begin{bmatrix} k_x & 0 \\ 0 & k_\theta \end{bmatrix} = \begin{bmatrix} 3707.760 & 0 \\ 0 & 0.221 \end{bmatrix} \quad (6)$$

The undamped equations of motion in matrix form are then:

$$M\ddot{q}(t) + Kq(t) = 0, \quad q(t) = \begin{bmatrix} x(t) \\ \theta(t) \end{bmatrix} \quad (7)$$

$$\begin{bmatrix} 0.43200 & 0.00710 \\ 0.00710 & 0.00078 \end{bmatrix} \begin{bmatrix} \ddot{x}(t) \\ \ddot{\theta}(t) \end{bmatrix} + \begin{bmatrix} 3707.760 & 0 \\ 0 & 0.221 \end{bmatrix} \begin{bmatrix} x(t) \\ \theta(t) \end{bmatrix} = 0 \quad (8)$$

The written component-wise,

$$\begin{cases} (m_p + m_c)\ddot{x} + m_c r \ddot{\theta} + k_x x = 0 \\ m_c r \ddot{x} + (m_c r^2 + J) \ddot{\theta} + k_\theta \theta = 0 \end{cases} \quad (9)$$

$$\begin{cases} 0.432\ddot{x} + 0.00710\ddot{\theta} + 3707.760x = 0 \\ 0.00710\ddot{x} + 0.00078\ddot{\theta} + 0.221\theta = 0 \end{cases} \quad (10)$$

To compute the natural frequencies of this system, the eigenproblem had to be solved, to do so a MATLAB code was used but the steps followed to find these frequencies will be explained on Appendix B. So, the values of the natural frequencies are:

$$w_{1n} = 16.7888 \frac{\text{rad}}{\text{s}} , \quad f_{1n} = 2.6720 \text{ Hz}$$

$$w_{2n} = 100.6990 \frac{\text{rad}}{\text{s}} , \quad f_{2n} = 16.0267 \text{ Hz}$$

The MATLAB script which has been run also computes the mode shapes for this MDOF system, these was the mode shape matrix.

$$\phi = \begin{bmatrix} \phi_{x1} & \phi_{x2} \\ \phi_{\theta 1} & \phi_{\theta 2} \end{bmatrix} = \begin{bmatrix} -0.0199 & -1.6495 \\ -35.6123 & 15.4260 \end{bmatrix} \quad (11)$$

The mode shapes describe how the platform and the cylinder move relative to each other at each natural frequency. The obtained mode shapes match the theoretical expectations for this system.

Since the elastic cord is much softer than the aluminum frame, the first mode naturally involves the rotation of the cylinder restrained mainly by the cord, while the platform moves slightly in phase. In contrast, the second mode corresponds to the lateral translation of the platform, dominated by the stiffness of the frame, with the cylinder moving out of phase. This behavior agrees with theory, as the lower-frequency mode is governed by the more compliant element (the cord), and the higher-frequency mode by the stiffer structural component (the frame).

3. Modal Test & Analysis

After having taken a clear picture of what would be expected out of the system in this experiment, this system was then tested in real life. The procedure by which this was done, along with the results and analysis of the SDOF and MDOF systems. This analysis will use the Line Fit Method to find the resonances present within the system. This was done as some datasets were not “clean” enough to find such resonances using the peak picking method. At the end of this chapter, the natural resonances of the system will be understood as performed in the lab.

3.1 Procedure

The experiment took the following steps:

1. The dimensions and mass of each component were measured
2. The experimental parameters were set in the program
 - a. Data would be collected for 10 seconds after a hit was registered
 - b. Force and acceleration would be sampled every $1/10^{\text{th}}$ of a second
 - c. Analysis would include frequencies from 0 to 2000 Hz
3. The accelerometer was attached:
 - a. On the side of the wood block for Part 1
 - b. On the middle of the cylinder for Part 2
 - c. The same location as Part 1 for the full system
4. The force hammer was then gently tapped against the tested part, generally next to the accelerometer
 - a. For the full set-up the middle of the cylinder was also tapped
5. 10 seconds were left, until the program indicated and another tap was made
6. This was done three times

3.2 SDOF Results & Analysis

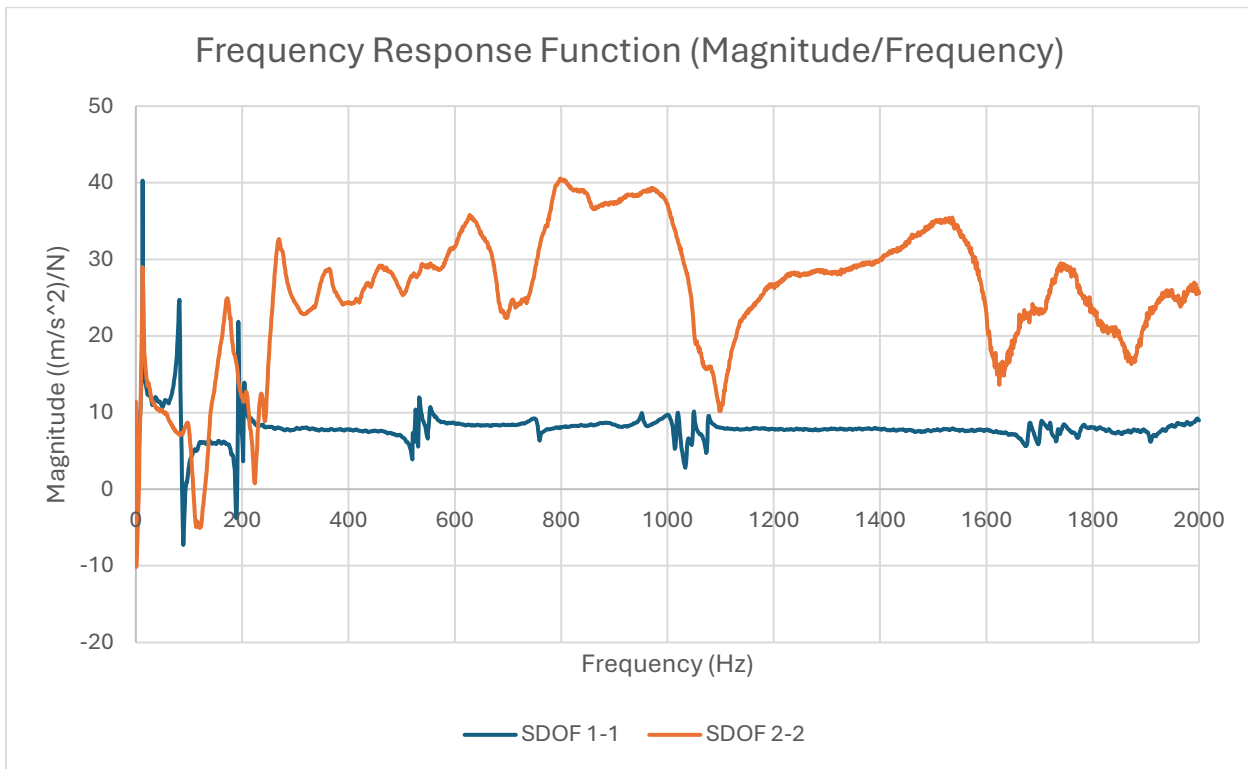


Figure 3 - The FRF of the two SDOF systems.

After carrying out this procedure the results of this can be seen in the frequency response graph of each part above. As can be seen, the FRF of Part 2 was much noisier than Part 1, especially after around 250 Hz. This is likely because the accelerometer only measured acceleration within the x plane of motion, not picking up the rotation the cylinder was experiencing. The analysis of the SDOF parts will focus on the region from 0 to 300 hertz, this will be as that is where the greatest regions of change occur.

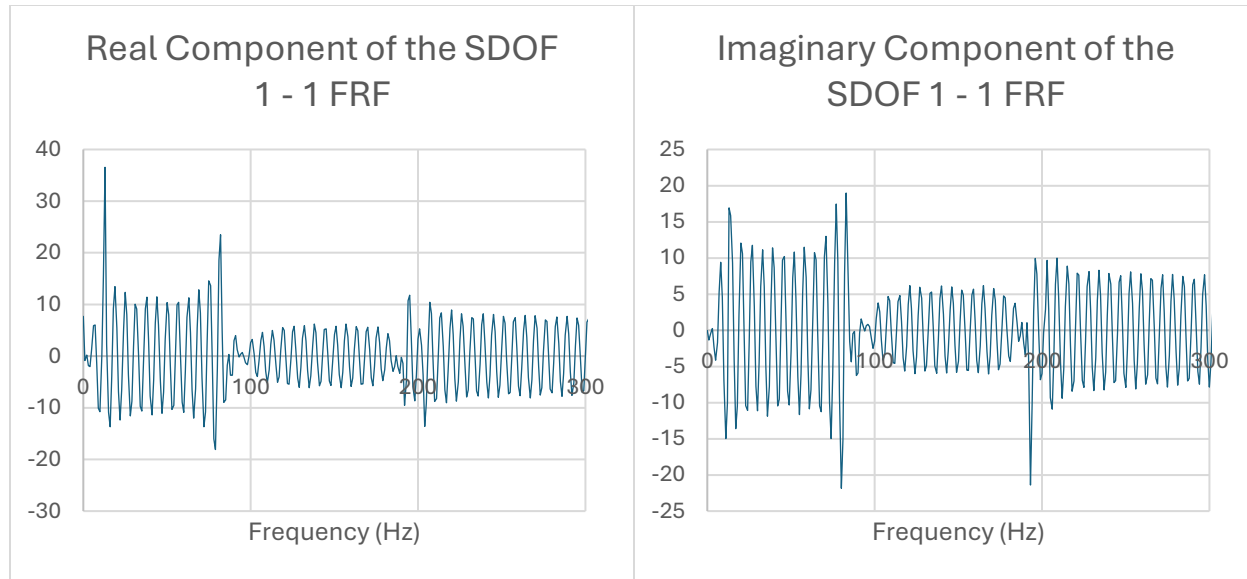


Figure 4 - The (Left) Real and (Right) Imaginary Component of the FRF for SDOF 1-1.

From the above FRF, the real and imaginary components could be found, these can be seen above for Part 1. These will be used, along with the FRFs, to identify frequency bands of interest. From this, the inverse FRF components can be found to perform the line fit method.

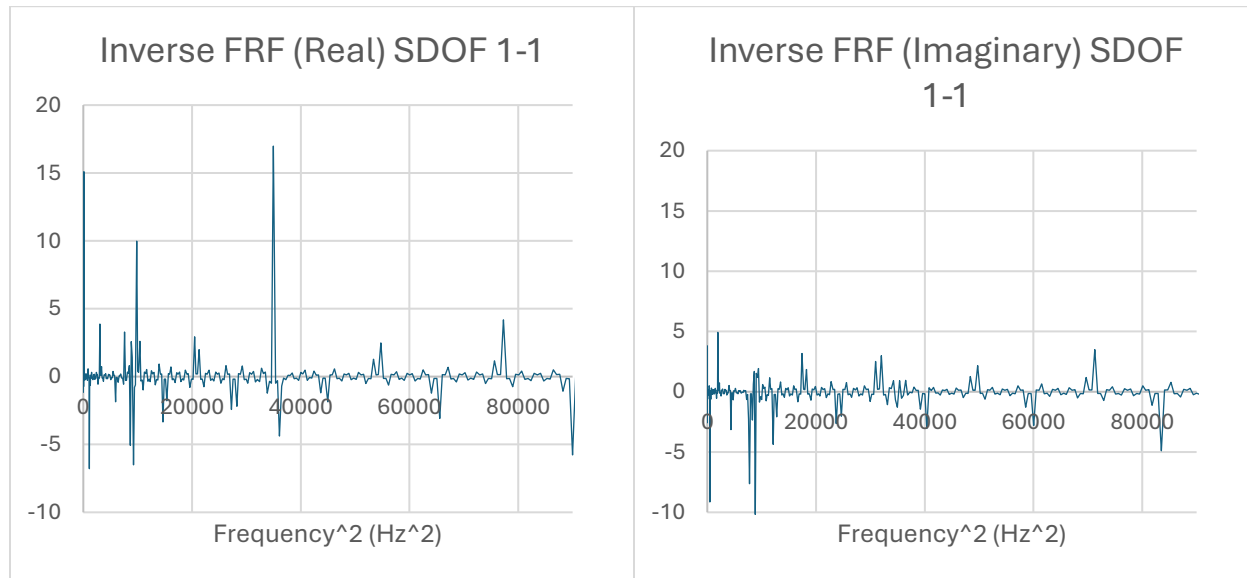


Figure 5 - The Inverse FRF graphs of the (Left) Real and (Right) Imaginary Components

These inverse graphs can be seen above, from these certain segments of interest (found using the previous FRFs) can be isolated and their lines of fit can be found. This was done for three segments for the SDOF systems and the results of that are in Appendix C. From these lines, resonances can be derived.

As the name of the method says, the aim is to find a line function that fits the curve, on the form $y = \mathbf{m}_R x + \mathbf{n}_R$ for the real part and $y = \mathbf{m}_I x + \mathbf{n}_I$ for the imaginary part.

With the four coefficients in bold, it is possible to find the natural frequencies for the three sections of each part with the formula:

$$\omega_r = \sqrt{\frac{-\mathbf{m}_R \mathbf{n}_R - \mathbf{m}_I \mathbf{n}_I}{\mathbf{n}_R^2 + \mathbf{n}_I^2}} \quad (12)$$

r is the number of segments into which the FRF has been divided.

At the end of the calculation, making a unit analysis, it was noticed that the result is in [1/Hz].

Table 1: Inverse of natural frequency values for SDOF functions

	$1/\omega_1[1/\text{Hz}]$	$1/\omega_2[1/\text{Hz}]$	$1/\omega_3[1/\text{Hz}]$
SDOF 1-1	0.083459	0.011055	0.00507
SDOF 2-2	0.069019	0.005698	0.003607

The result has been inverted to obtain the correct values for the natural frequencies:

Table 2: Natural frequency values for SDOF functions

	$\omega_1[\text{Hz}]$	$\omega_2[\text{Hz}]$	$\omega_3[\text{Hz}]$
SDOF 1-1	11.9819	90.45793	197.2243
SDOF 2-2	14.48881	175.4984	277.2043

3.3 MDOF Results & Analysis

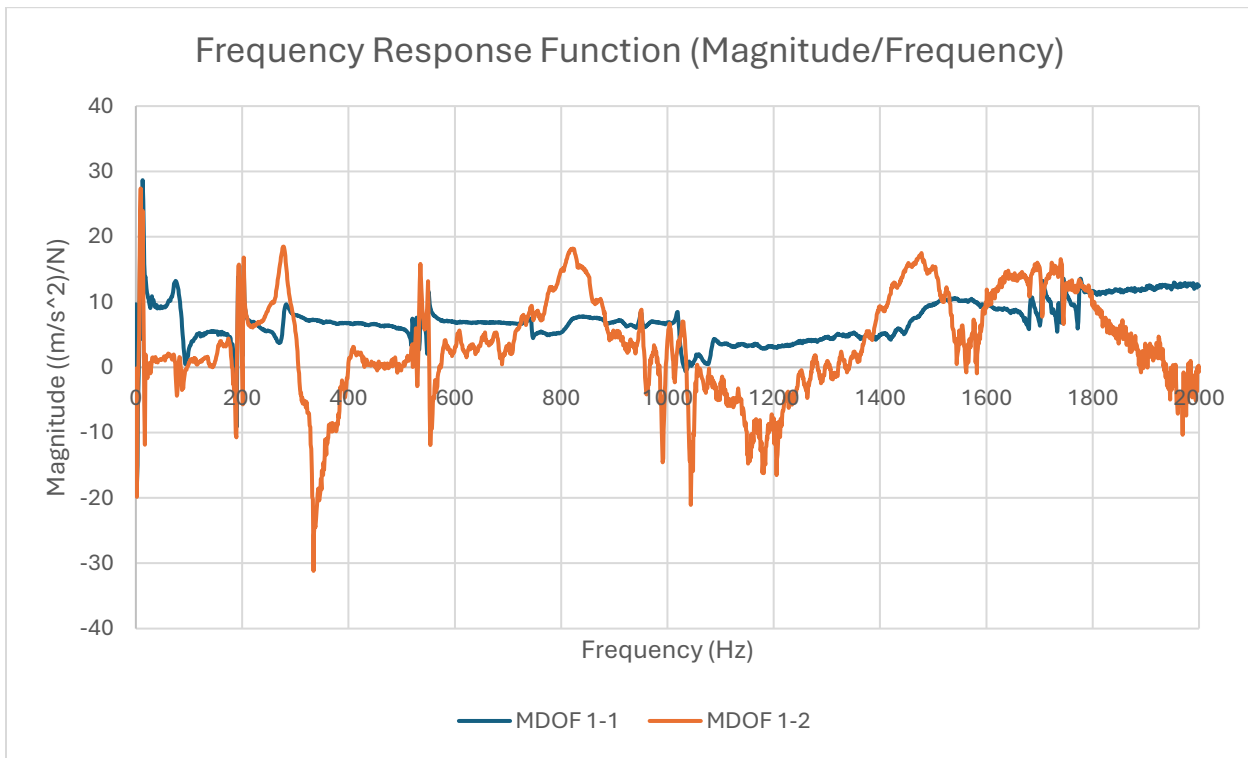


Figure 6 - The FRF of the two measurements of the MDOF system.

The first part of the MDOF Analysis follows the same process as the SDOF analysis. The FRF of the full system can be seen above for the two trials, both measured at location one but excited at location one and two. Much like the SDOF experiment, the measurements involving the rotating cylinder are very noisy, likely for the aforementioned reason. Additionally, there are some similarities between this graph and the respective SDOF graphs. The two measurement sets also line up in notable locations, indicating areas which should be analyzed further. The band from 0 to 600 Hz was analyzed. Much like the SDOF analysis:

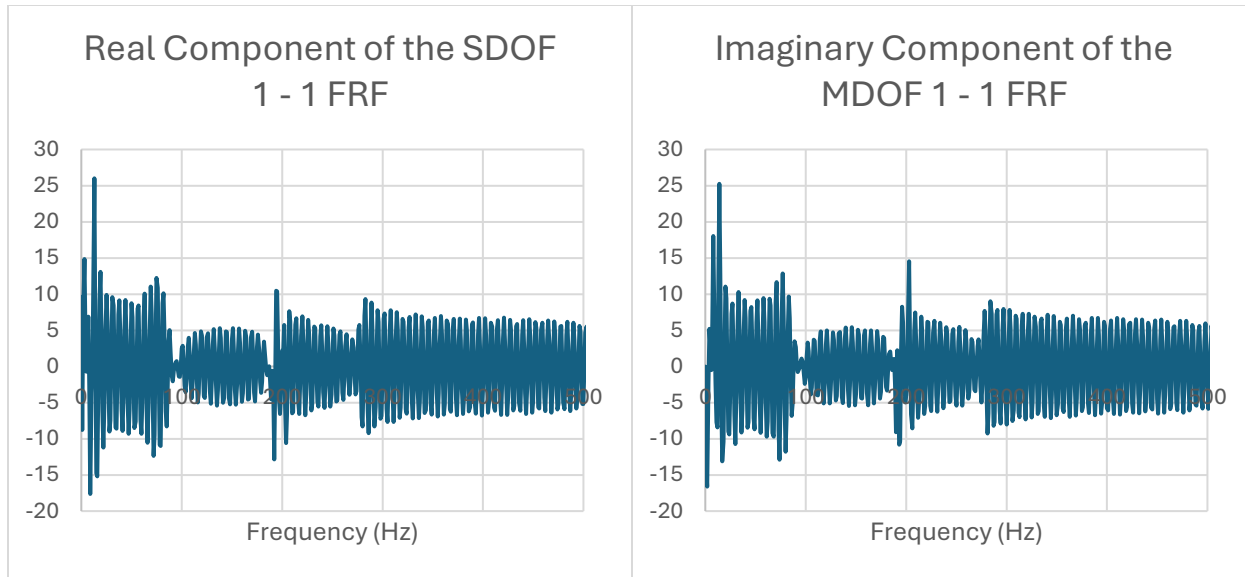


Figure 7 - The (Left) Real and (Right) Imaginary Component of the FRF for MDOF 1-1.

The real and imaginary components were found.

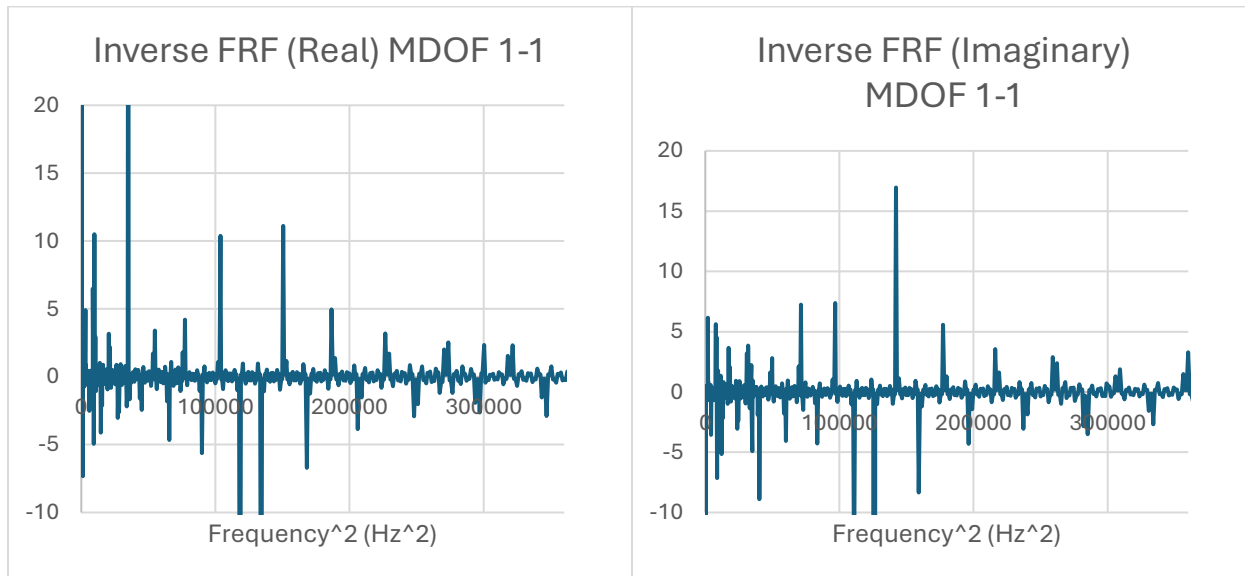


Figure 8 - The Inverse FRF graphs of the (Left) Real and (Right) Imaginary Components

Inverse graphs were made, and the respective lines of fitness were found. There were five relevant bands analyzed in total, they are in Appendix C, along with all graphs in Appendix D.

Table 3: Inverse of natural frequency values for MDOF functions

	$\omega_1[1/\text{Hz}]$	$\omega_2[1/\text{Hz}]$	$\omega_3[1/\text{Hz}]$	$\omega_4[1/\text{Hz}]$	$\omega_5[1/\text{Hz}]$
MDOF 1-1	0,05985	0,008961	0,005057	0,004689	0,004212
MDOF 1-2	0,108334	0,004923	0,003003	0,001866	0,001985

Table 4: Natural frequency values for MDOF functions

	$\omega_1[\text{Hz}]$	$\omega_2[\text{Hz}]$	$\omega_3[\text{Hz}]$	$\omega_4[\text{Hz}]$	$\omega_5[\text{Hz}]$
MDOF 1-1	16,70836	111,5889	197,7648	213,2657	237,4428
MDOF 1-2	9,230748	203,1146	332,989	535,9795	503,9029

The inverse of the natural frequencies and then natural frequencies, for each segment, for both the functions were found, with the formula (12).

4. Discussion

Having found the natural frequencies of the S and MDOF systems in theory and in practice, these results can now be discussed. This will be done in this chapter, first discussing the final results of the experiment and then comparing those results with the theoretical natural frequencies of the systems.

Three relevant bands were found for the two SDOF systems and five for the MDOF system, this gave three and five potential natural frequencies respectively. What can be seen between the SDOF and MDOF results is that the SDOF frequencies follow over to the MDOF system. This can be observed most clearly from the SDOF 1-1 to MDOF 1-1. In both there are apparent frequency pairs:

- 11.98 & 16.71 Hz
- 90.46 & 111.59 Hz
- 197.22 & 197.76 (or 213.27) Hz

These three (though the 90.46 & 111.59 Hz is not as close) frequency pairs show the elements of the SDOF components influence the MDOF system. This can also be seen from the SDOF 2-2 results from 14.49 & 16.71 Hz and 277.20 & 237.44 Hz. Additionally, there are some patterns seen in the MDOF 1-2 results, though less so. These are:

- 11.98 or 14.49 & 9.23 Hz from both SDOF components
- 197.22 & 203.1 Hz from SDOF 1-1
- 277.20 & 332.99 Hz from SDOF 2-2

These relations are much weaker however, and there seems to be no input for the 503.90 and 535.98 Hz results. The reasons for this could stem from the much higher noise seen in the results, likely as a product of the cylinder's motion. The mismatch between SDOF and MDOF frequencies may also be due to interference between the SDOF natural frequencies which causes changes.

When compared with the theoretical expectations there is some similarity. The calculated SDOF 1-1 natural frequency of 17.606 Hz is close to that of the measured 11.98 Hz. The same goes for the expected MDOF frequency of 16.053 Hz, which lines up very well with the MDOF 1-1 frequency of 16.71. Though the other expected frequency of 2.672 Hz is not seen in the experimental results.

This could be due to any number of issues, the nature of the experiment may have eliminated the possibility of such a low frequency, the accelerometer may not have picked it up, or nearby frequencies drowned it out. Additionally, the high frequency values found during the experiment may be due to unexpected complexity in the system (maybe the various

connections between parts), disturbances in the surrounding environment, or issues with the experiment/analysis.

Overall, some similarities can be seen between the theoretical and experimental results, though there is visible mismatch between the expected and derived results. The experimental results seemed to support the assumption that the SDOF component frequencies contribute to the MDOF system natural frequencies.

5. Conclusion

The objectives of this laboratory were to model, analyze, and experimentally verify the dynamic behavior of both a single-degree-of-freedom (SDOF) and a multiple-degree-of-freedom (MDOF) mechanical system. The theoretical study successfully predicted the undamped natural frequencies and corresponding mode shapes based on the measured geometrical and mechanical properties. Experimentally, the modal tests confirmed that the SDOF components significantly influence the MDOF system behavior, with comparable resonant frequencies appearing in both setups.

Although discrepancies were observed between theoretical and experimental values—mainly due to measurement noise, damping effects, and simplifications in the analytical model—the general trends aligned with expectations. The lower-frequency mode was governed by the elastic cord and dominated by the cylinder's rotation, while the higher-frequency mode was associated with the frame stiffness and platform translation. Overall, the results validated the theoretical modeling approach and demonstrated how coupled oscillatory behavior can be accurately predicted through fundamental dynamic analysis.

Appendix A – Component Dimensions & Mass

Table 5 - The dimensions & mass of each component of the system.

Platform	
Length (cm):	14.5
Width (cm):	15
Height (cm):	1.9
Mass (kg):	0.188
Aluminum Supports	
Length (cm):	1.6
Width (cm):	0.2
Height (cm):	21.2
Mass (kg):	0.0755
Cylinder	
External Diameter (cm):	11
Inner Diameter (cm)	10.1
Height (cm):	10
Mass (kg):	0.129
Sensor Sensitivities	
Force Hammer (mV/N):	21.12
Accelerometer (mV/(m/s ²)):	10.62

Appendix B – Theoretical Calculation

Calculation for the aluminum beams weight

→ Volume for 1 beam (V_b):

$$V_b = 1.6 \times 21.2 \times 0.2 = 6.784 \text{ cm}^3 \quad (12)$$

$$\text{Aluminum's density } (\rho_{Al}) = 2.7 \frac{\text{g}}{\text{cm}^3}$$

→ Weight for the Aluminum beams:

$$m_b = V_b \times \rho_{Al} \times 4 \quad (13)$$

$$m_b = 6.784 \times 2.7 \times 4 \times \frac{1}{1000} = 0.072 \text{ kg} \quad (14)$$

Calculation for platform weight

Total weight of the frame (m_f)= 0.678 kg

Weight of the platform (m_p):

$$m_p = \frac{m_f - m_b}{2} \quad (15)$$

$$m_p = \frac{0.678 - 0.072}{2} = 0.303 \text{ kg} \quad (16)$$

Calculation for frame's stiffness (k_x)

To compute the platform's stiffness, an analysis of the DOF for the frame needs to be done. The platform will have lateral translation on the axe x, according to Figure 2. Each leg behaves as a vertical beam vent by the platform's lateral motion. Bending axis is the weak axis of the rectangular leg section.

Since the legs are clamped to the base and to a stiff platform, they are considered as fixed-fixed columns. For top lateral translation, the lateral stiffness per leg.

$$k_{leg} = \frac{12 EI}{L^3} \quad (17)$$

The young's modulus for aluminum is 69 GPa, and with the following formula the second moment of area about the bending axes (I) for a rectangle will be calculated.

$$I = \frac{bh^3}{12} = \frac{0.016(0.002)^3}{12} = 1.067 \times 10^{-11} \text{ m}^4 \quad (18)$$

$$k_{leg} = \frac{12 \times 69 \times 10^9 \times 1.067 \times 10^{-11}}{0.212^3} = 926.940 \text{ N/m} \quad (19)$$

For the 4 beams.

$$k_x = k_{leg} \times 4 = 956.940 \times 4 = 3707.760 \text{ N/m} \quad (20)$$

Calculation for k_s and k_θ

The stiffness of the elastic cord was obtained from a static elongation test, in which two different masses were hung vertically to measure the corresponding extensions. So, with the following formula the stiffness of the cord was obtained.

$$k_s = \frac{\Delta F}{\Delta x} = \frac{(m_2 - m_1) \times g}{x_2 - x_1} = \frac{(0.685 - 0.007) \times 9.81}{0.266 - 0.175} = 73.09 \text{ N/m} \quad (21)$$

When the cylinder rotates by a small angle, the point on its surface at radius r , moves a distance L , $\Delta L = r\theta$. The elastic cord resists that motion, creating a restoring torque on the cylinder. This torque-angle relationship defines an equivalent torsional stiffness. The following formula was used to convert from the linear stiffness of the cord to the torsional stiffness.

$$k_\theta = k_s r^2 = 73.09 \times (0.055^2) = 0.221 \text{ N/m} \quad (22)$$

Calculation for natural frequency for SDOF

With the values of the frame stiffness and the platform's mass, the natural frequency of the SDOF can be computed.

$$w_n = \sqrt{\frac{k_x}{m_p}} = \sqrt{\frac{3707.760}{0.303}} = 110.62 \frac{\text{rad}}{\text{s}} \quad ; \quad f_n = \frac{w_n}{2\pi} = \frac{110.62}{2\pi} = 17.61 \text{ Hz}$$

Calculation for M matrix

Once the generalized coordinates are defined, the kinematics of the MDOF can be defined as.

- Cylinder center translation: $u(t) = x(t) + r\theta(t)$
- Velocities: $\dot{u} = \dot{x} + r\dot{\theta}$

So, the formula for Kinetic Energy is the following:

$$T = \frac{1}{2}m_p\dot{x}^2 + \frac{1}{2}m_c(\dot{x} + r\dot{\theta})^2 + \frac{1}{2}J\dot{\theta}^2 \quad (23)$$

$$T = \frac{1}{2}m_p\dot{x}^2 + \frac{1}{2}m_c(\dot{x}^2 + 2\dot{x}r\dot{\theta} + r^2\dot{\theta}^2) + \frac{1}{2}J\dot{\theta}^2 \quad (24)$$

$$T = \frac{1}{2}(m_p + m_c)\dot{x}^2 + (m_c r)\dot{\theta}\dot{x} + \frac{1}{2}\dot{\theta}^2(r^2 m_c + J) \quad (25)$$

By definition:

$$T = \frac{1}{2}\dot{q}^T M \dot{q} \quad (26)$$

So,

$$M = \begin{bmatrix} m_p + m_c & m_c r \\ m_c r & m_c r^2 + J \end{bmatrix} \quad (27)$$

The cylinder used for the MDOF has been considered as a thin-walled cylinder since the following condition was accomplished, and the thickness of the wall did not have a significant effect on the results.

$$\frac{R_{int}}{R_{ext}} \geq 0.9 \quad (28)$$

$$\frac{0.051}{0.055} = 0.928 \quad (29)$$

So, the inertia of the cylinder is the following one:

$$J = m_c R_{ext}^2 \quad (30)$$

So, M matrix will be the following one:

$$M = \begin{bmatrix} 0.303 + 0.129 & 0.129 \times 0.055 \\ 0.129 \times 0.055 & 0.129 \times 0.055^2 + 0.129 \times 0.055^2 \end{bmatrix} = \begin{bmatrix} 0.432 & 0.00710 \\ 0.00710 & 0.00078045 \end{bmatrix} \quad (31)$$

Calculation for undamped equations of motion for the MDOF

The following formula will show how to get the written component-wise for the equations of motion for the MDOF from the matrix form.

$$M\ddot{q} + Kq = 0 \quad (32)$$

$$\begin{bmatrix} m_p + m_c & m_c r \\ m_c r & m_c r^2 + J \end{bmatrix} \begin{bmatrix} \ddot{x}(t) \\ \ddot{\theta}(t) \end{bmatrix} + \begin{bmatrix} k_x & 0 \\ 0 & k_\theta \end{bmatrix} \begin{bmatrix} x(t) \\ \theta(t) \end{bmatrix} = \begin{bmatrix} 0 \\ 0 \end{bmatrix} \quad (33)$$

$$\begin{bmatrix} \ddot{x}(m_p + m_c) + \ddot{\theta}(m_c r) \\ \ddot{x}(m_c r) + \ddot{\theta}(m_c r^2 + J) \end{bmatrix} + \begin{bmatrix} k_x x \\ k_\theta \theta \end{bmatrix} = \begin{bmatrix} 0 \\ 0 \end{bmatrix} \quad (34)$$

Then, each row of this matrix is divided to one equation each, as the following system.

$$\begin{cases} (m_p + m_c)\ddot{x} + m_c r \ddot{\theta} + k_x x = 0 \\ m_c r \ddot{x} + (m_c r^2 + J) \ddot{\theta} + k_\theta \theta = 0 \end{cases} \quad (35)$$

Calculation to compute the undamped natural frequencies

The undamped natural frequencies of the coupled system are found by solving the generalized eigenvalue problem.

$$(K - w^2 M)\phi = 0 \quad (36)$$

$$\det(K - w^2 M) = 0 \quad (37)$$

To simplify the steps followed the following nomenclature will be established.

$$M = \begin{bmatrix} m_p + m_c & m_c r \\ m_c r & m_c r^2 + J \end{bmatrix} = \begin{bmatrix} a & b \\ b & c \end{bmatrix} \quad (38)$$

So,

$$\det(K - w^2 M) = \begin{vmatrix} k_x - w^2 a & -w^2 b \\ -w^2 b & k_\theta - w^2 c \end{vmatrix} = 0 \quad (39)$$

$$(k_x - w^2 a)(k_\theta - w^2 c) - (w^2 b)^2 = 0 \quad (40)$$

Collect powers of w^2 , let ($x = w^2$).

$$(ac - b^2)x^2 - (k_x c + k_\theta a)x + k_x k_\theta = 0 \quad (41)$$

That's a quadratic in $x = w^2$. So, the quadratic is solved.

$$w_{1,2}^2 = (k_x c + k_\theta a) \pm \frac{\sqrt{(k_x c + k_\theta a)^2 - 4k_x k_\theta (ac - b^2)}}{2(ac - b^2)} ; \quad f_{1,2} = \frac{w_{1,2}}{2\pi} \quad (42)$$

Solving this, the values for the natural frequencies from section 2.4. are computed.

MATLAB script

```

1 %> z=DF Platform + Cylinder (undamped) - Build M, K, and Natural Frequencies
2 %> q = [1 x 1];
3 %> q = [1 x 1];
4 %> theta : Platform lateral translation [m]
5 %> theta : cylinder rotation about its center [rad]
6 clear; clc;
7 %> -----
8 %> Masses ----- GIVEN / MEASURED DATA -----
9 %> M_p = 0.303; % [kg] platform mass
10 M_c = 0.102; % [kg] cylinder mass
11 m_c = 0.007; % [kg] frame stiffness in x
12 m_s = 2.87700000; % [N/m] frame stiffness in z
13 k_x = 1000000; % [N/m] lateral stiffness from your geometry/orientation
14 R_ext = 0.055; % [m] inner radius (181 mm dia -> 0.0585 m)
15 R_int = 0.045; % [m] outer radius
16 R_eff = R_int; % [m] effective wrap/contact radius for the cord
17 %> R_eff = R_ext;
18 %> R_eff = R_ext;
19 %> R_eff = R_ext;
20 %> R_eff = R_ext;
21 %> R_eff = R_ext;
22 %> R_eff = R_ext;
23 %> R_eff = R_ext;
24 %> R_eff = R_ext;
25 %> R_eff = R_ext;
26 g = 9.81; % [m/s^2]
27 m_1 = 0.007; % [kg] first mass (7 g)
28 m_2 = 0.102; % [kg] second mass (102 g)
29 L1 = (22.5 - 5.0)/1000; % [m] length with m1 (22.5cm - 5cm)
30 L2 = (31.0 - 5.0)/1000; % [m] length with m2 (31.0cm - 5cm)
31 dF = (m2 * m1) / (g); % [N] force difference
32 dF = dF * 1000; % [N] force difference
33 dL = dF / dL; % [m/m] axial stiffness of the single continuous cord
34 k_axial = dF / dL; % [Nm/rad]
35 %> k_theta = k_axial * pi^2; % [Nm/rad]
36 %> k_theta = k_axial * pi^2; % [Nm/rad]
37 k_theta = k_axial * pi^2; % [Nm/rad]
38 %> -----
39 %> BUILD M AND K MATRICES -----
40 %> Mass matrix:
41 M = [ m_p m_c; m_c m_s ];
42 M = M + C_p; %> M_p + M_c
43 M = M + C_z; %> M_c + C_z
44 M = M + C_theta; %> M_c + C_theta
45 %> Stiffness matrix:
46 K = [ 0 0 0; 0 0 0; 0 0 0 ];
47 K = K + k_axial * I_3;
48 K = K + k_theta * J_3;
49 K = [ K; 0; 0 ];
50 K = [ 0; K; 0 ];
51 %> -----
52 %> PRINT EQUATIONS OF MOTION -----
53 fprintf('Undamped equations of motion (matrix form):\n');
54 fprintf(' [M](q_dot_dot) + [K](q) = {0}, with q = [x; theta]\n\n');
55 disp('q = [ ]'); disp(M);
56 disp('q_dot = [ ]'); disp(W);
57 disp('q_dot_dot = [ ]'); disp(K);
58 %> -----
59 %> NATURAL FREQUENCIES -----
60 %> Solve generalized eigenproblem: (K - w^2 M) phi = 0
61 [Phi, D] = eig(K, M); % D is diag(w^2)
62 w1 = sqrt(diag(D)); % [rad/s]

```

Figure 9. MATLAB script

Appendix C – Line Fit Method Analysis Functions

1. SDOF Trial 1-1

Frequency Band 1 (0 – 15 Hz)			
m_R	n_R	m_I	n_I
0.0107	-1.165	-0.00765	-0.310
Frequency Band 2 (62 – 102 Hz)			
m_R	n_R	m_I	n_I
0.000309	-2.837	-0.000376	2.756
Frequency Band 3 (173 – 213 Hz)			
m_R	n_R	m_I	n_I
0.000285	-11.106	-3.924*10^-5	1.415

2. SDOF Trial 2-2

Frequency Band 1 (7 – 20 Hz)			
m_R	n_R	m_I	n_I
0.000793	-0.161	-0.000779	0.168
Frequency Band 2 (167 – 185 Hz)			
m_R	n_R	m_I	n_I
5.997*10^-5	-1.933	-3.931*10^-5	1.054
Frequency Band 3 (261 – 283 Hz)			
m_R	n_R	m_I	n_I
2.020*10^-5	-1.621	-1.825*10^-5	1.318

3. MDOF Trial 1-1

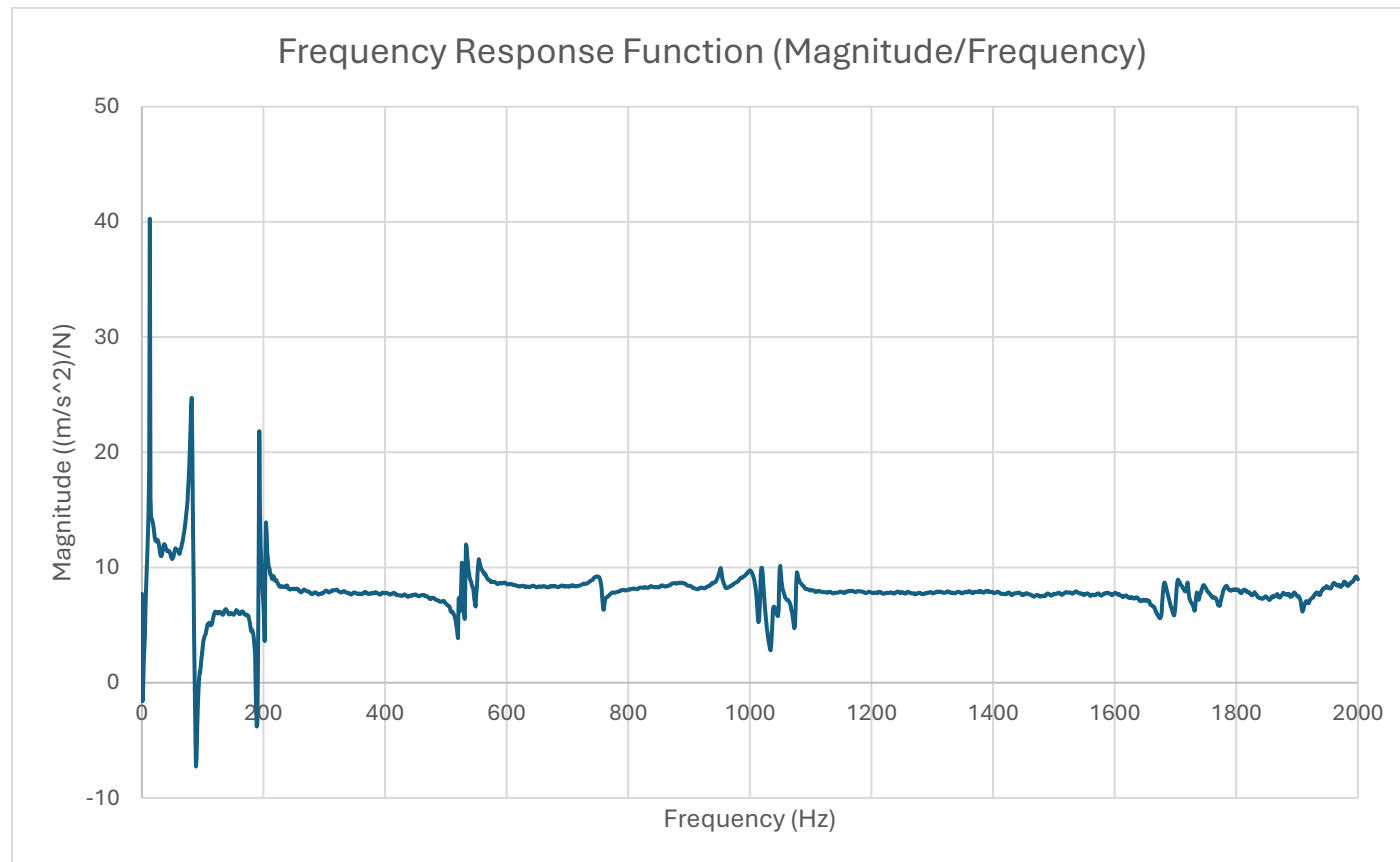
Frequency Band 1 (0 – 20 Hz)			
m_R	n_R	m_I	n_I
0.00162	-0.481	-0.000969	0.204
Frequency Band 2 (69 – 105 Hz)			
m_R	n_R	m_I	n_I
0.000561	-6.337	-0.000134	3.040
Frequency Band 3 (181 – 198 Hz)			
m_R	n_R	m_I	n_I
0.000398	-15.657	-0.000471	18.377
Frequency Band 4 (198 – 216 Hz)			
m_R	n_R	m_I	n_I
8.465*10^-5	-3.727	-1.734*10^-5	1.179
Frequency Band 5 (267 – 292 Hz)			
m_R	n_R	m_I	n_I
9.464*10^-5	-8.045	-6.697*10^-5	2.020*10^-5

4. MDOF Trial 1-2

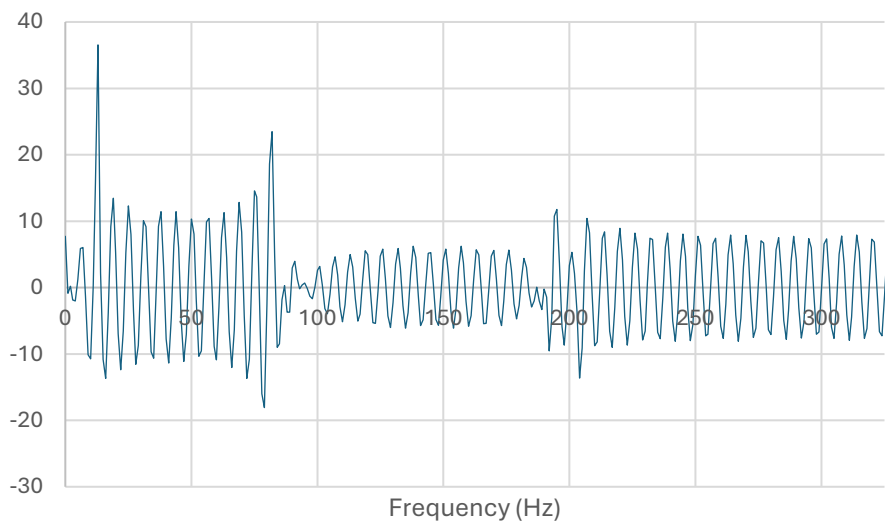
Frequency Band 1 (0 – 28 Hz)			
m_R	n_R	m_I	n_I
0.00871	-0.746	-0.00262	0.211
Frequency Band 2 (196 – 212 Hz)			
m_R	n_R	m_I	n_I
8.826	-3.654	-8.653×10^{-5}	3.557
Frequency Band 3 (323 – 339 Hz)			
m_R	n_R	m_I	n_I
7.939×10^{-5}	-8.915	-5.786×10^{-5}	6.256
Frequency Band 4 (529 – 540 Hz)			
m_R	n_R	m_I	n_I
8.887×10^{-5}	-25.862	0.000112	-31.838
Frequency Band 5 (543 – 557 Hz)			
m_R	n_R	m_I	n_I
0.000115	-36.544	-5.912×10^{-5}	18.051

Appendix D – All Analysis Graphs

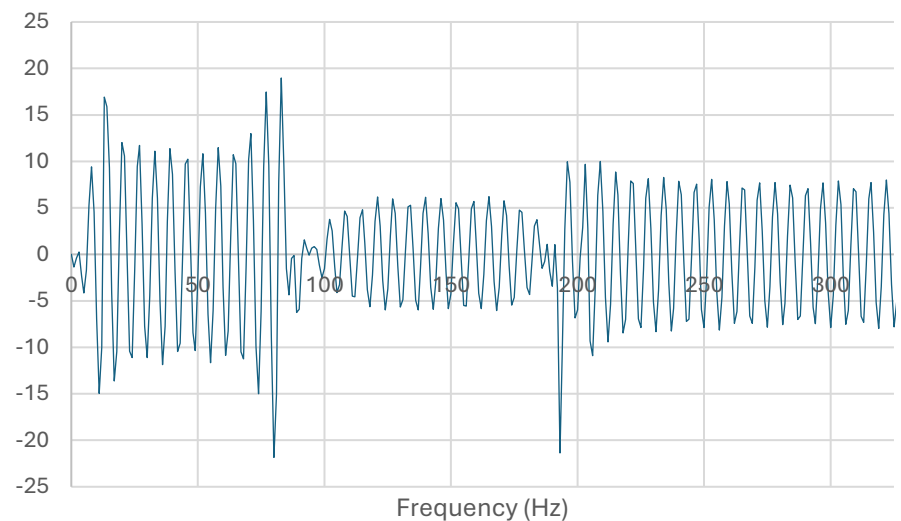
1. SDOF 1-1



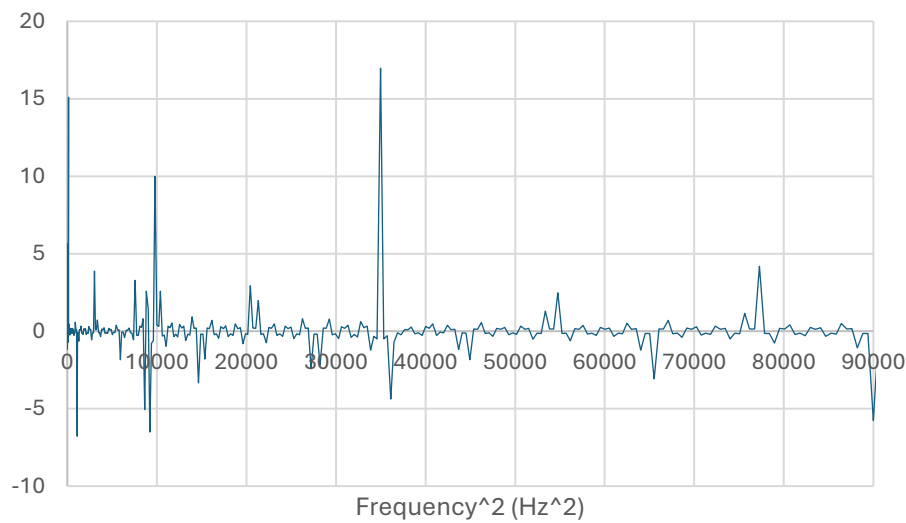
Real Component of the SDOF 1 - 1 FRF



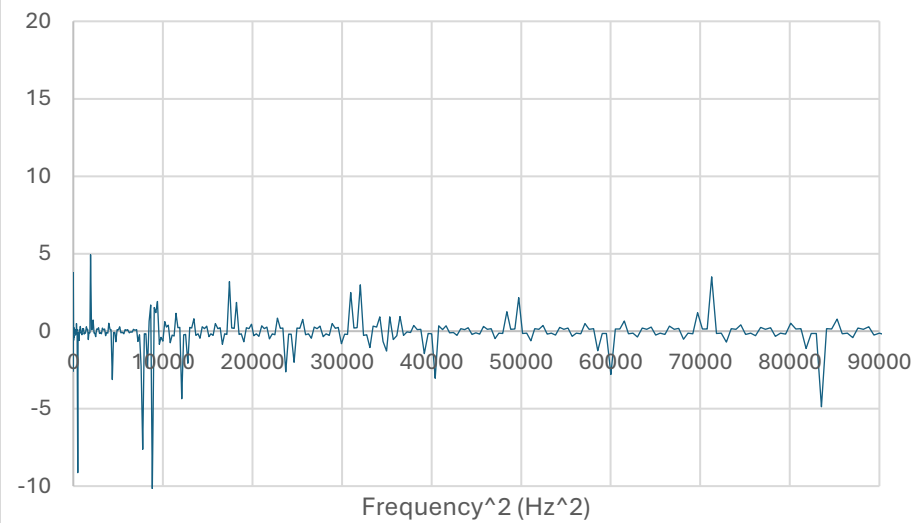
Imaginary Component of the SDOF 1 - 1 FRF



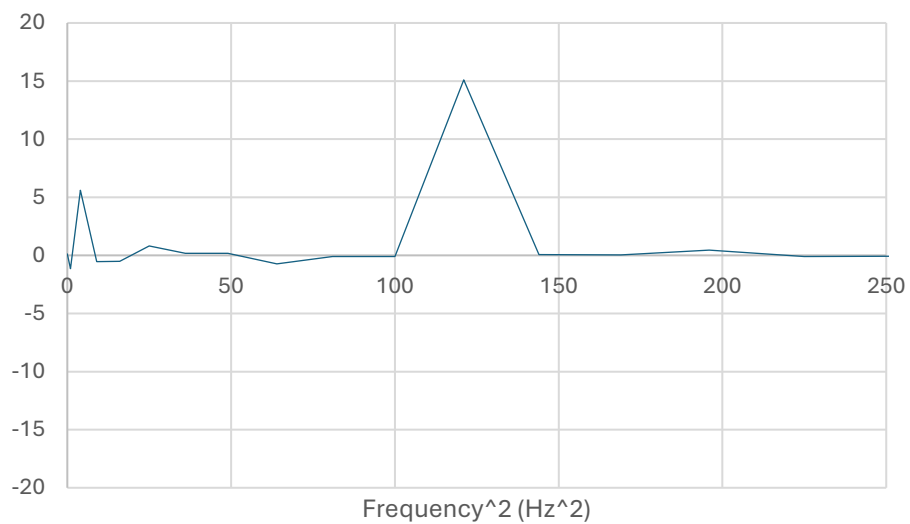
Inverse FRF (Real) SDOF 1-1



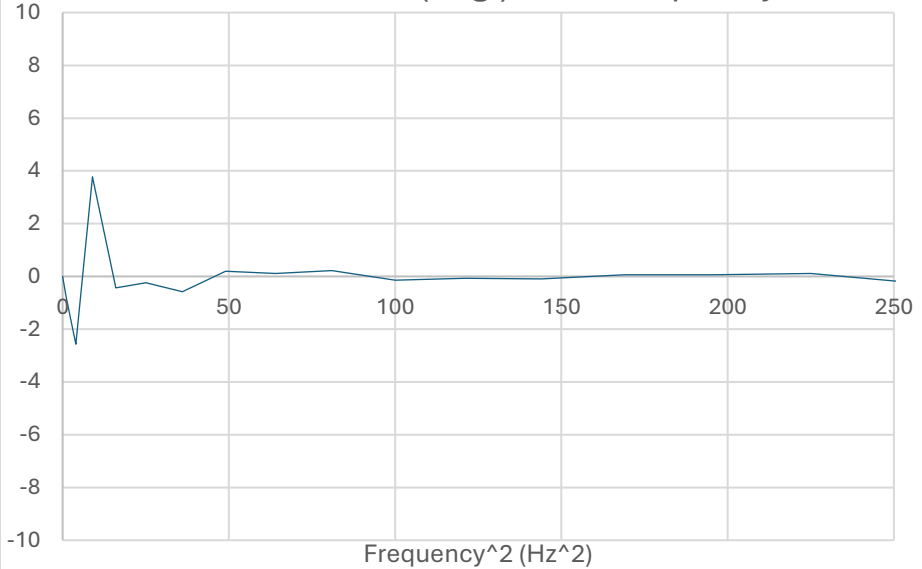
Inverse FRF (Imaginary) SDOF 1-1



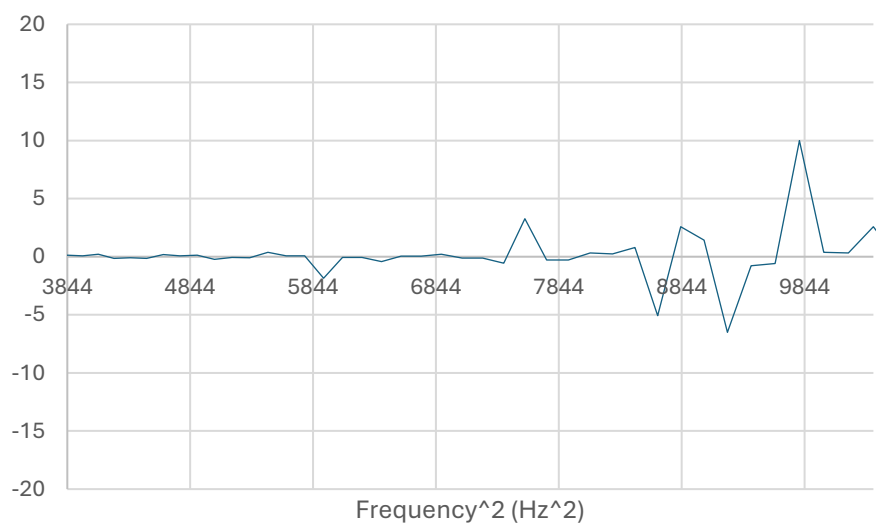
SDOF 1-1 Inverse (Real) FRF - Frequency 1



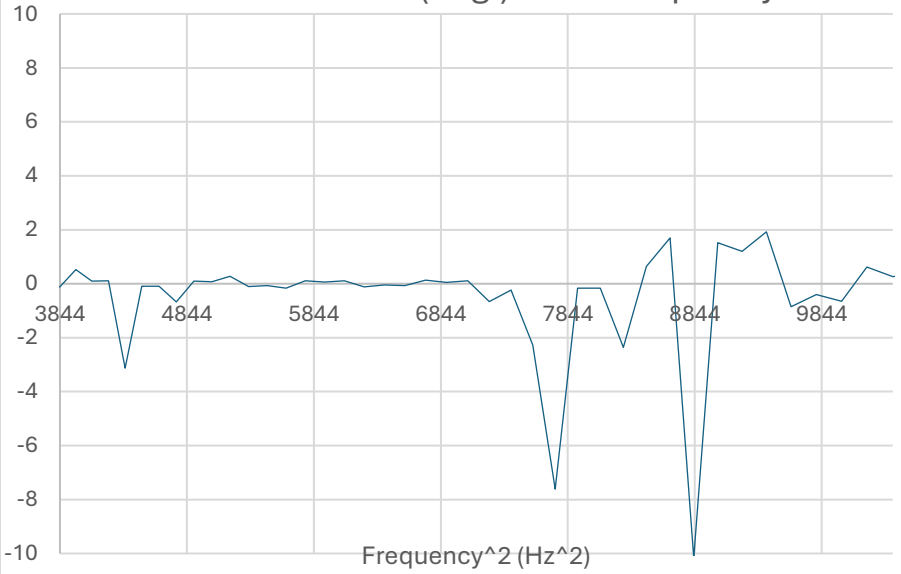
SDOF 1-1 Inverse (Img.) FRF - Frequency 1



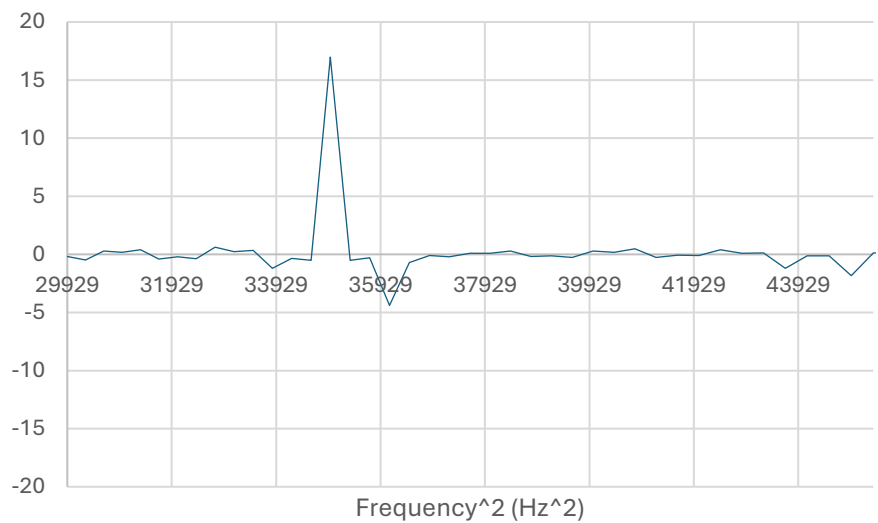
SDOF 1-1 Inverse (Real) FRF - Frequency 2



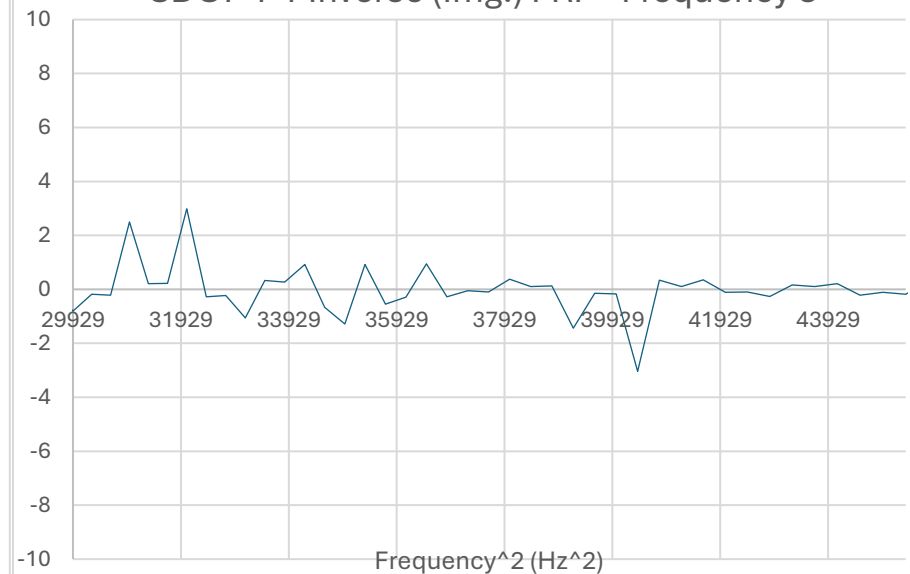
SDOF 1-1 Inverse (Img.) FRF - Frequency 2



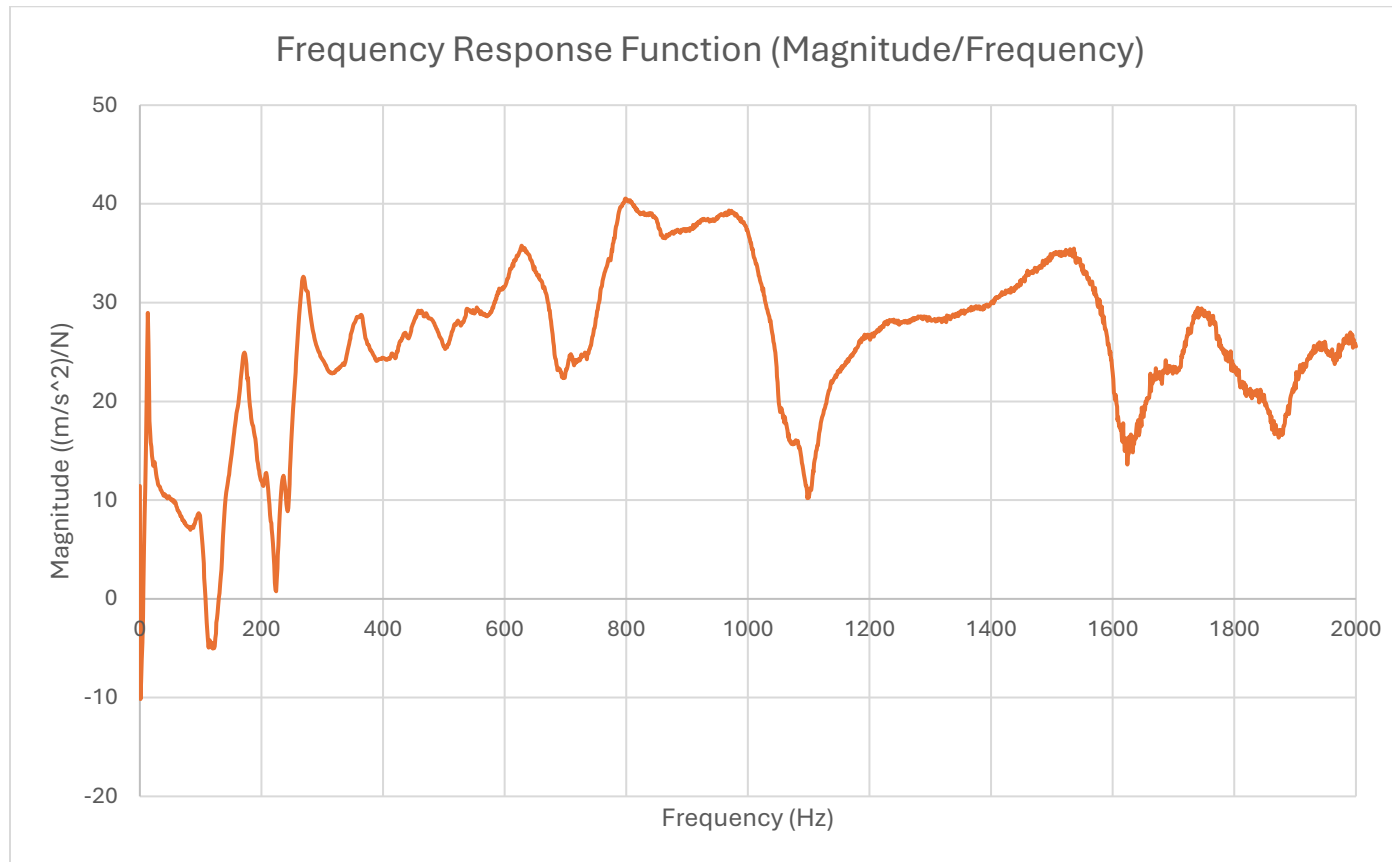
SDOF 1-1 Inverse (Real) FRF - Frequency 3



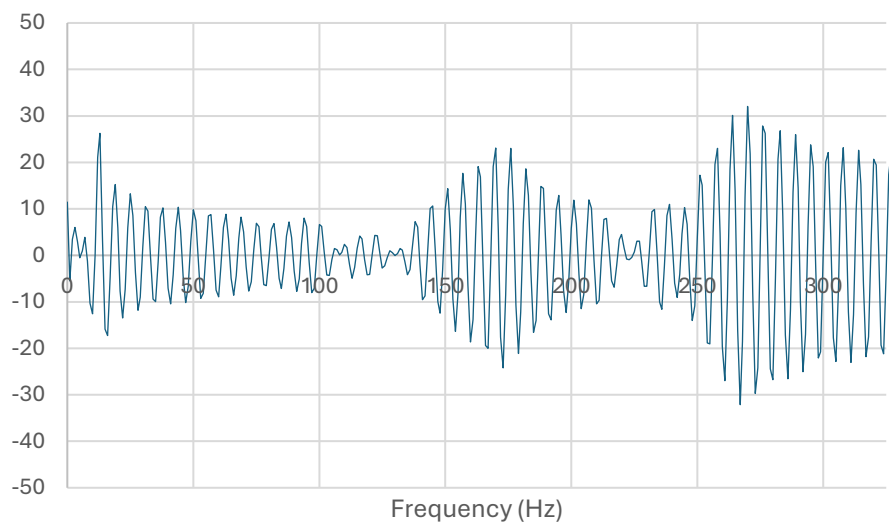
SDOF 1-1 Inverse (Img.) FRF - Frequency 3



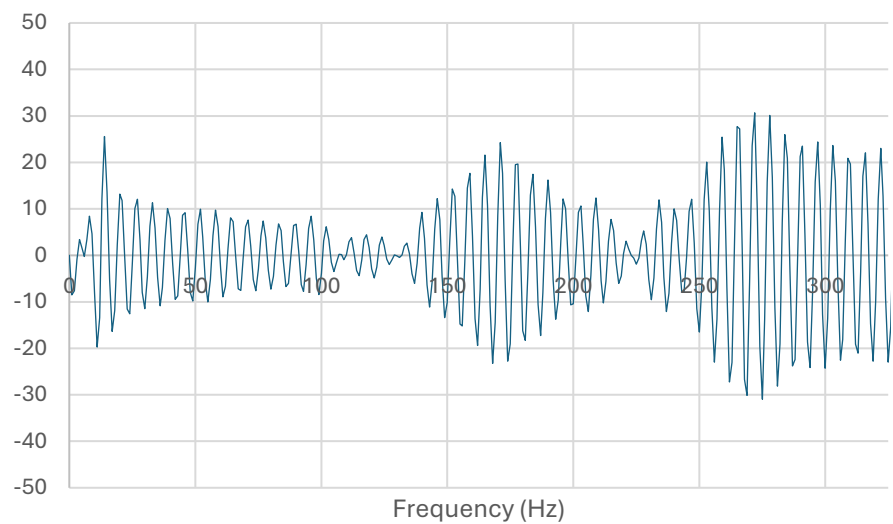
2. SDOF 2-2



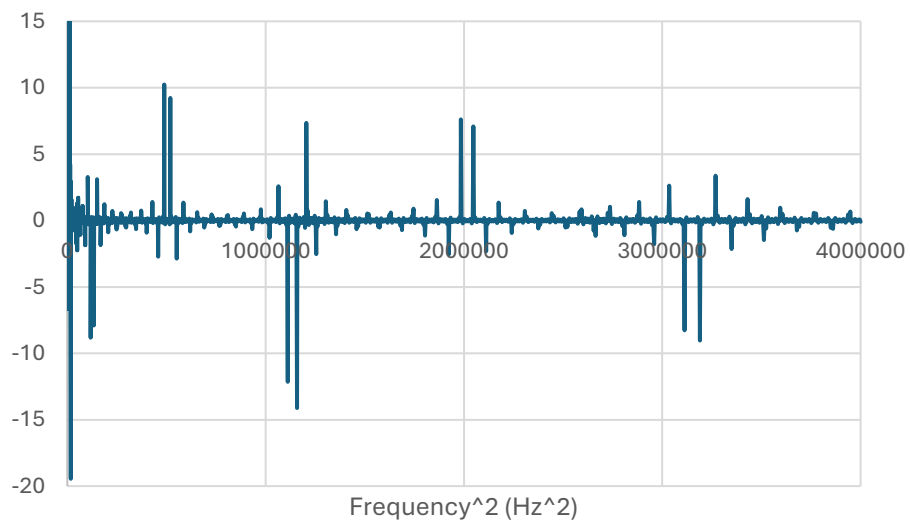
Real Component of the SDOF 2 - 2 FRF



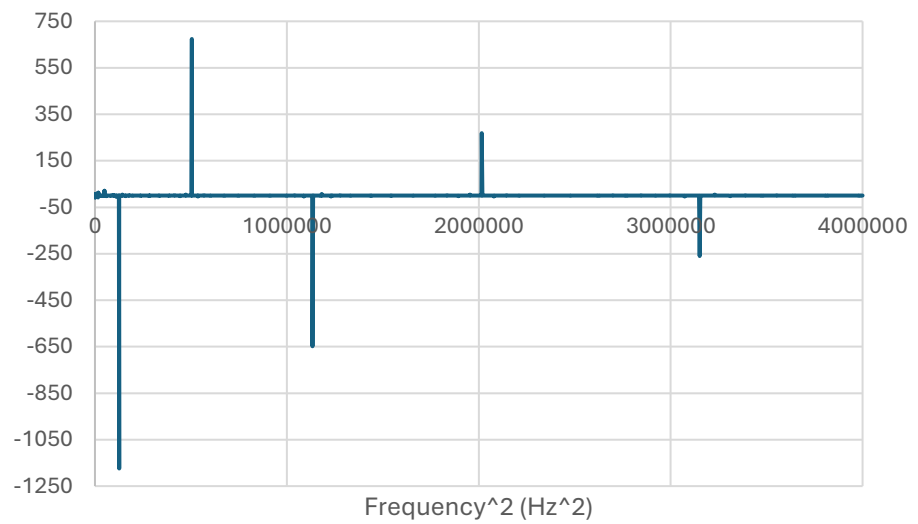
Imaginary Component of the SDOF 2 - 2 FRF



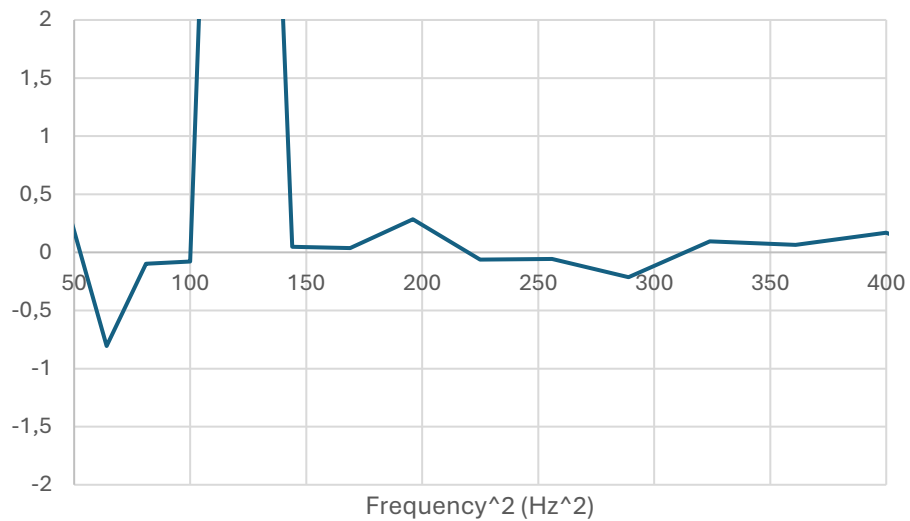
Inverse FRF (Real) SDOF 2-2



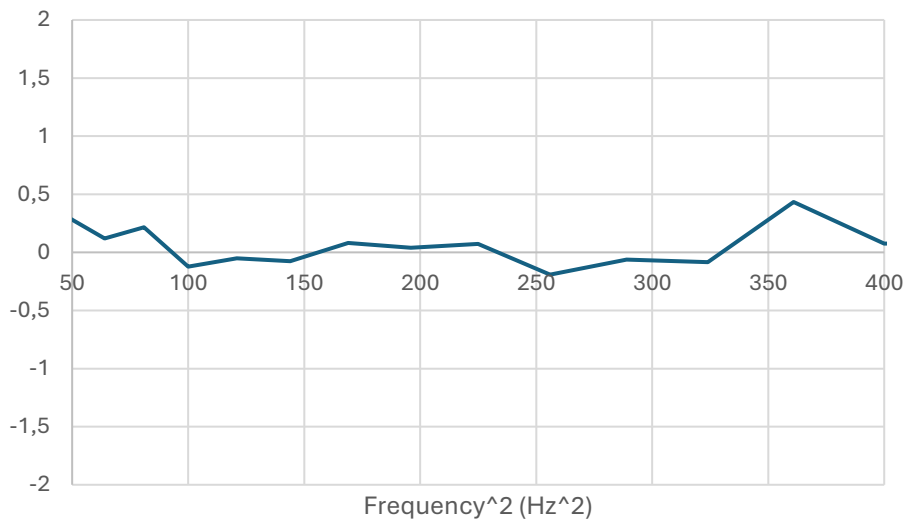
Inverse FRF (Imaginary) SDOF 2-2



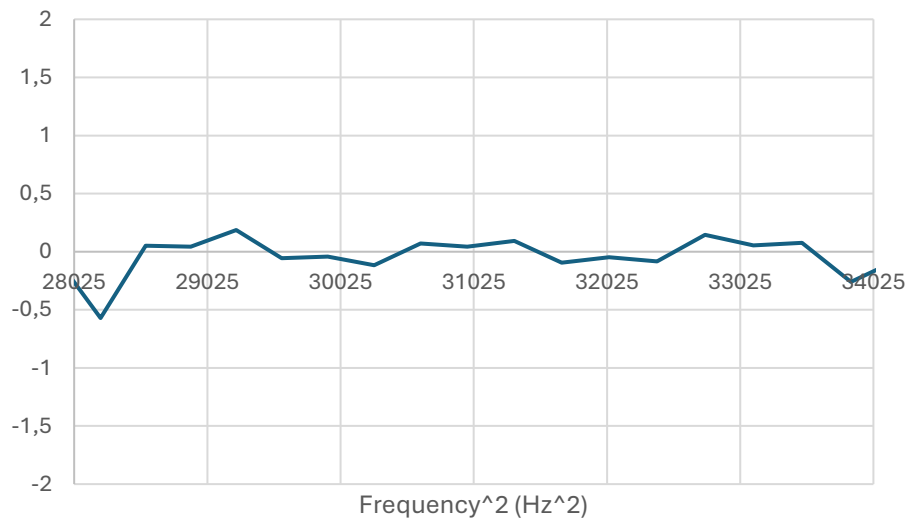
SDOF 2-2 Inverse (Real) FRF - Frequency 1



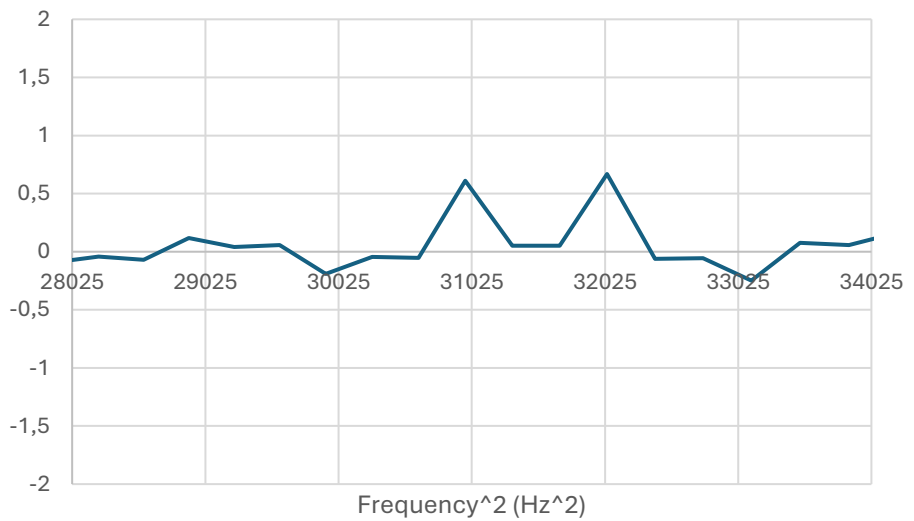
SDOF 2-2 Inverse (Img) FRF - Frequency 1



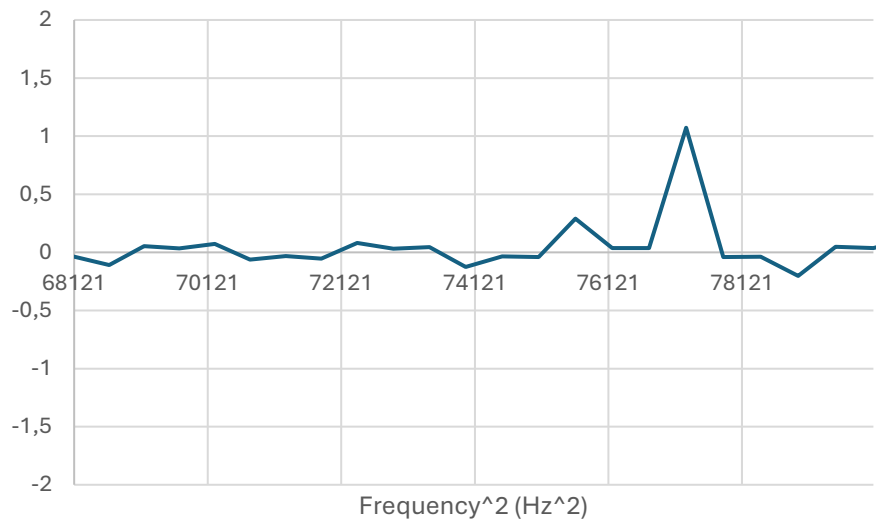
SDOF 2-2 Inverse (Real) FRF - Frequency 2



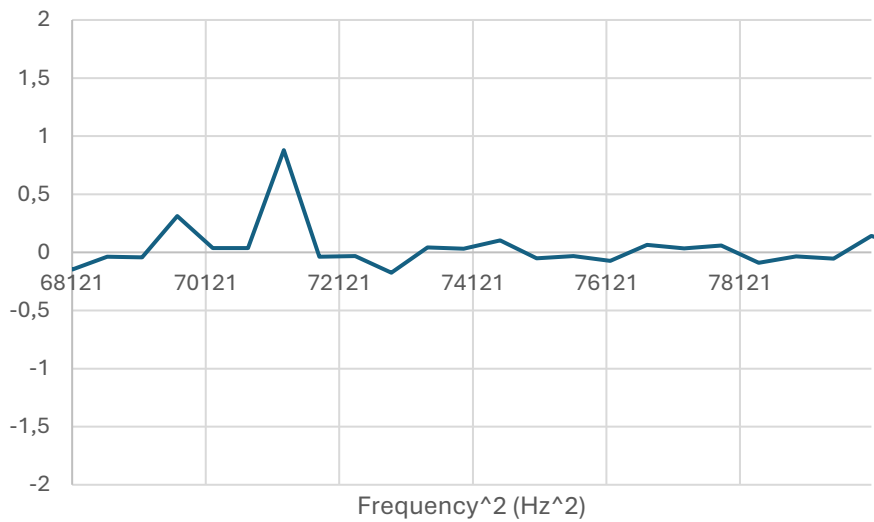
SDOF 2-2 Inverse (Img) FRF - Frequency 2



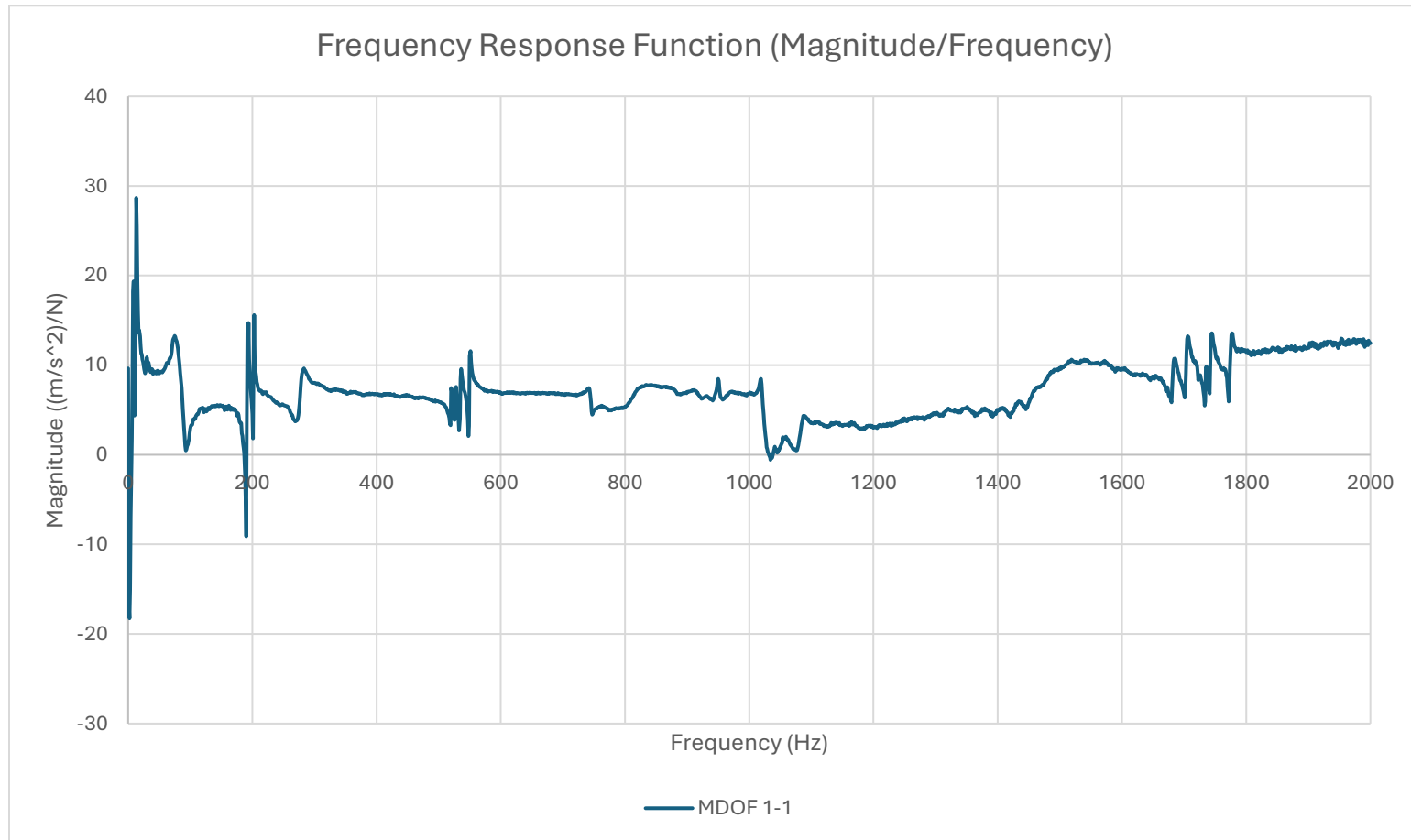
SDOF 2-2 Inverse (Real) FRF - Frequency 3



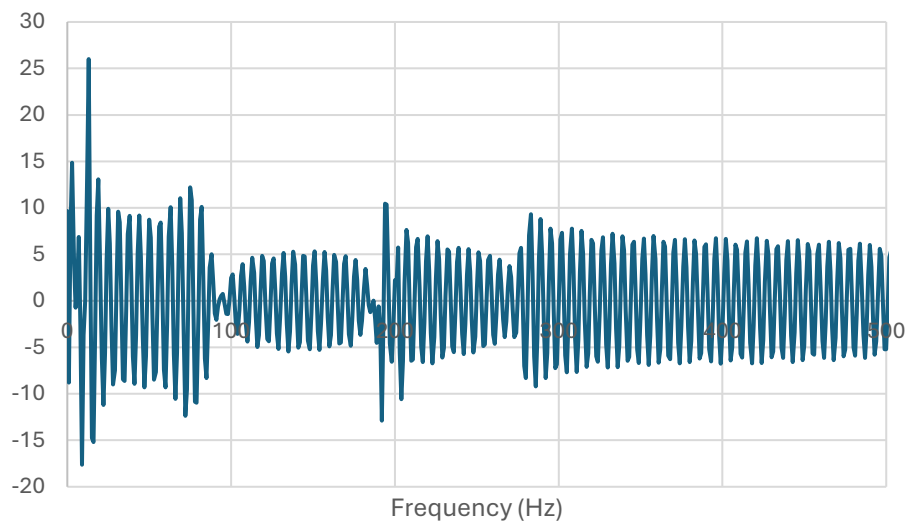
SDOF 2-2 Inverse (Img) FRF - Frequency 3



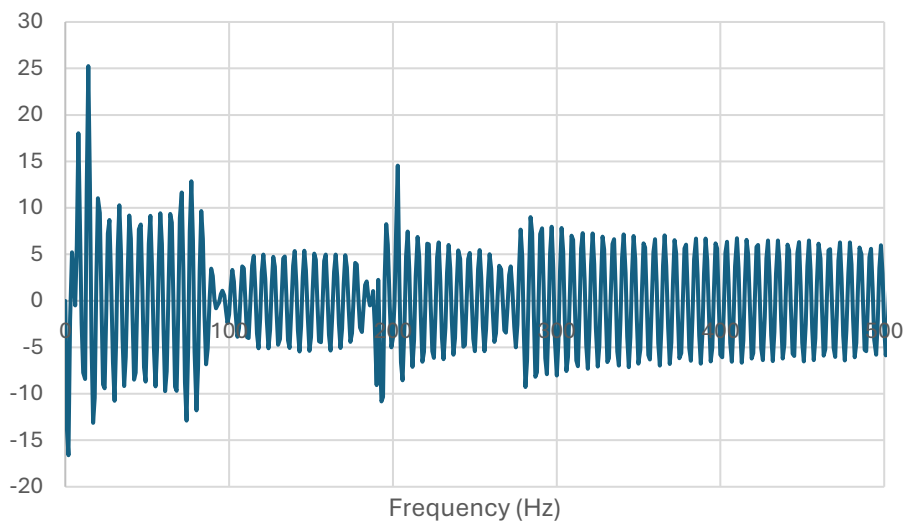
2. MDOF 1-1



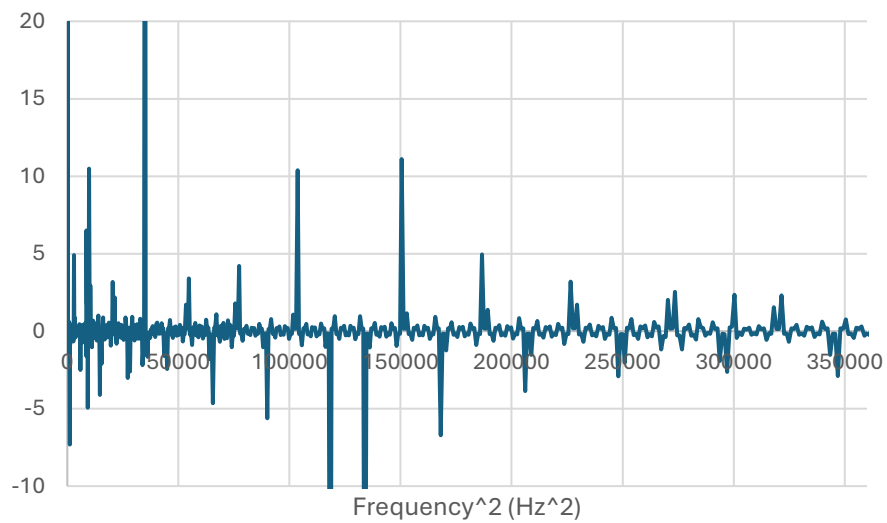
Real Component of the MDOF 1 - 1 FRF



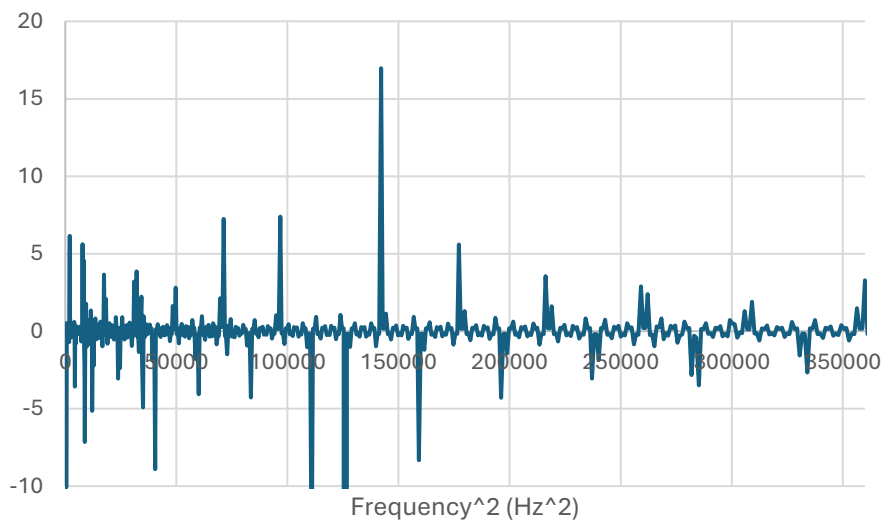
Imaginary Component of the MDOF 1 - 1 FRF



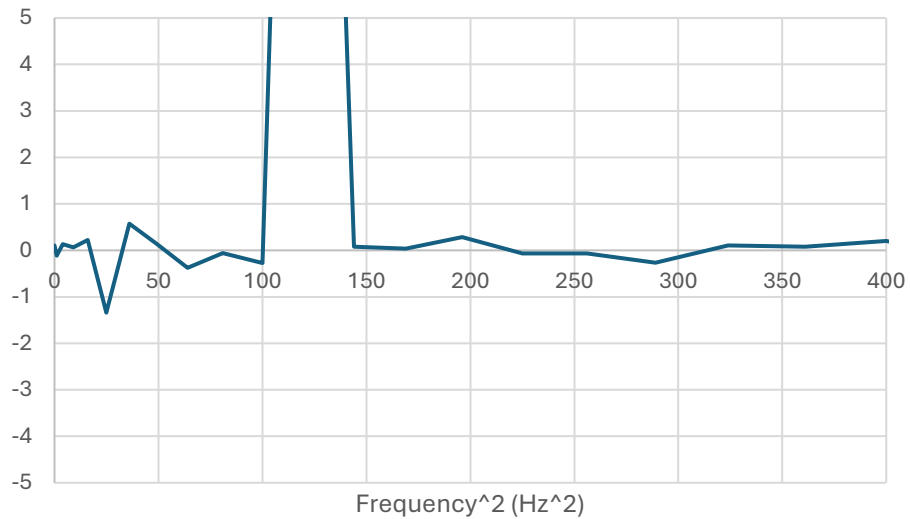
Inverse FRF (Real) MDOF 1-1



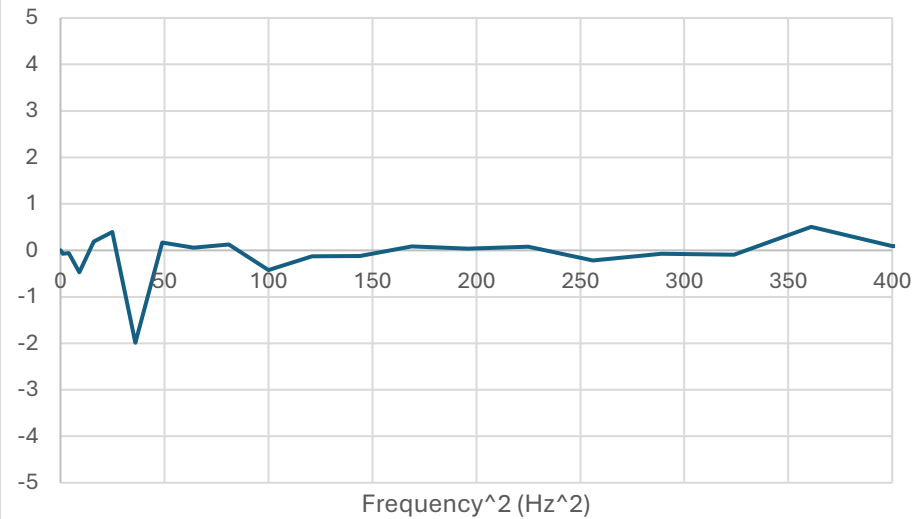
Inverse FRF (Imaginary) MDOF 1-1



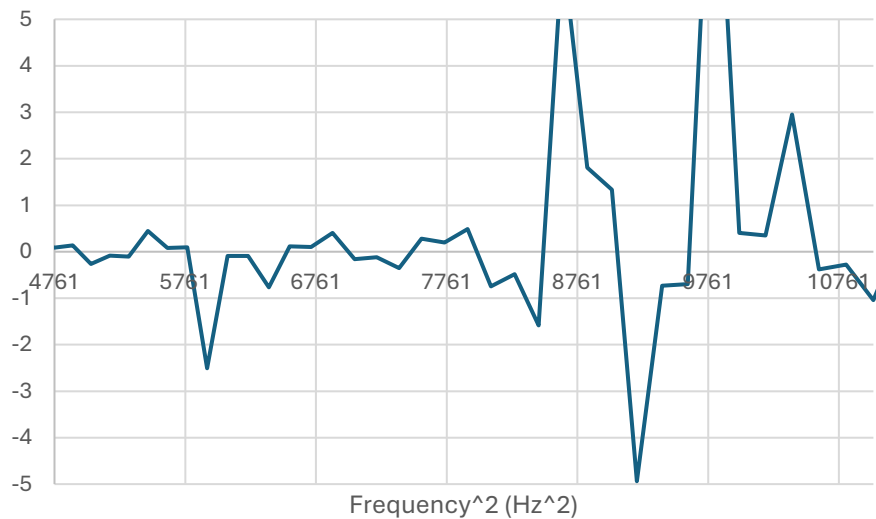
MDOF 1-1 Inverse (Real) FRF - Frequency 1



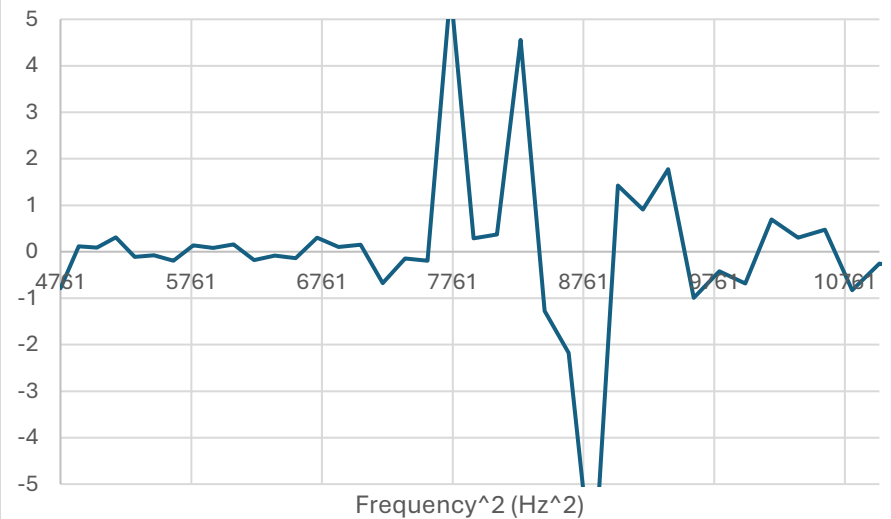
MDOF 1-1 Inverse (Img.) FRF - Frequency 1



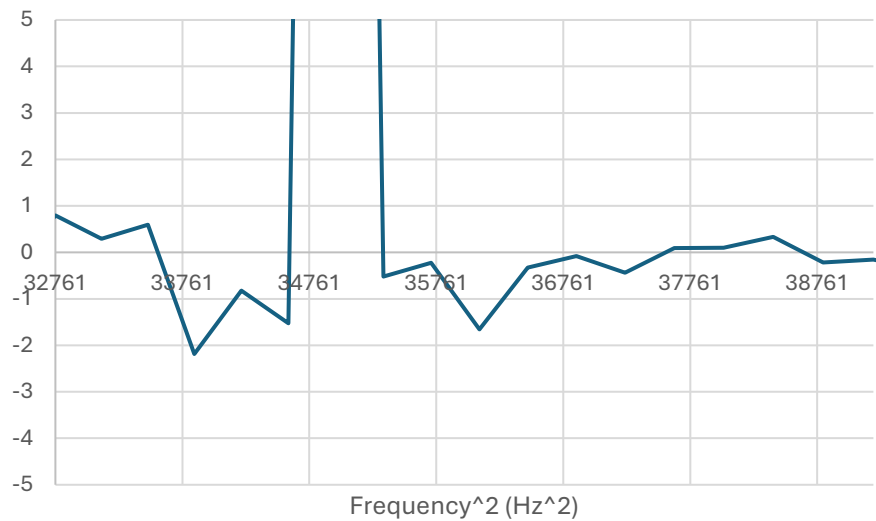
MDOF 1-1 Inverse (Real) FRF - Frequency 2



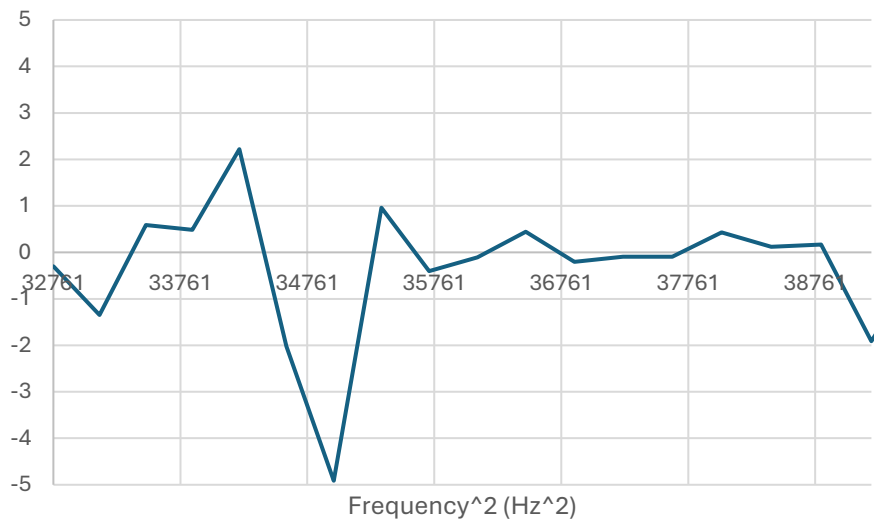
MDOF 1-1 Inverse (Img.) FRF - Frequency 2



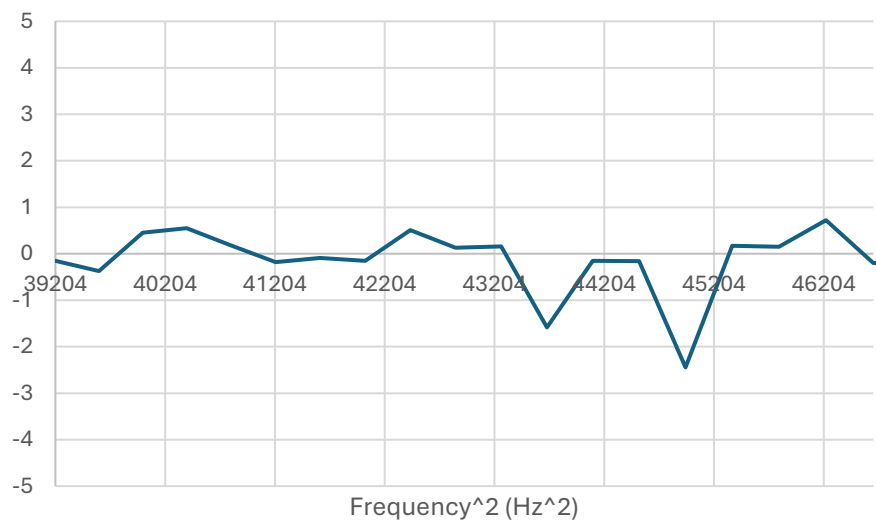
MDOF 1-1 Inverse (Real) FRF - Frequency 3



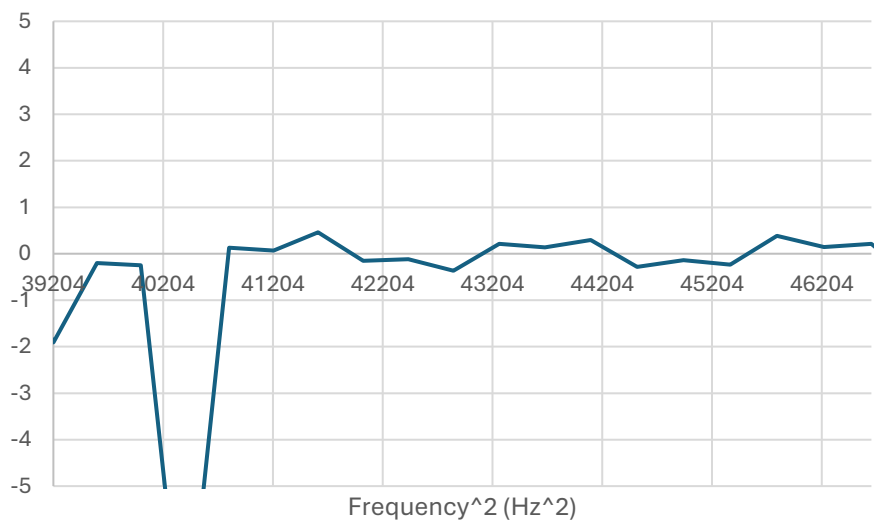
MDOF 1-1 Inverse (Img.) FRF - Frequency 3



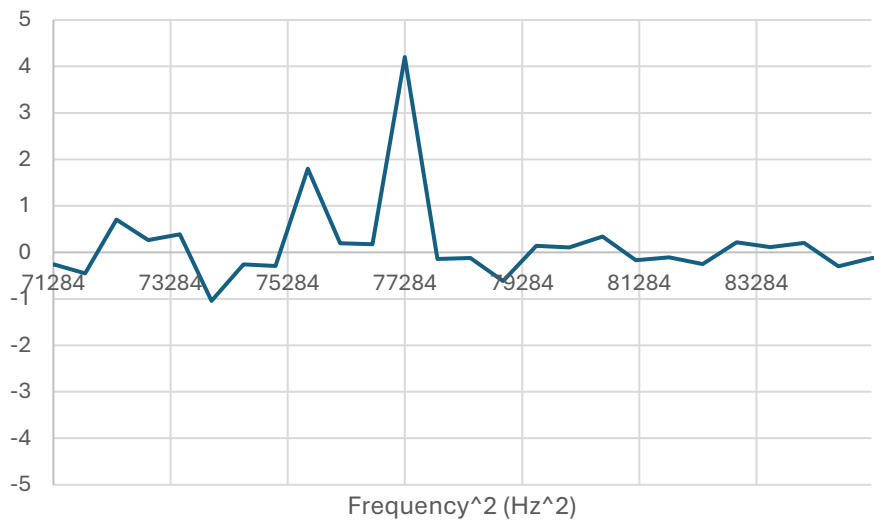
MDOF 1-1 Inverse (Real) FRF - Frequency 4



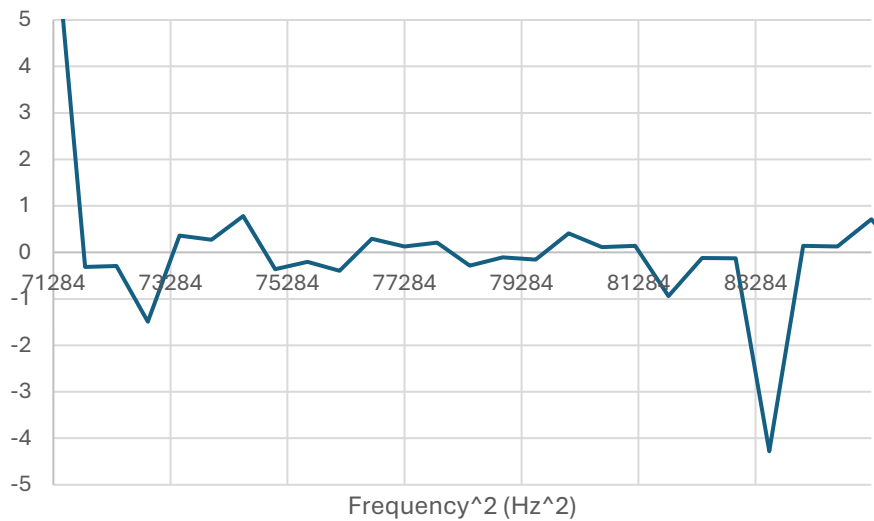
MDOF 1-1 Inverse (Img.) FRF - Frequency 4



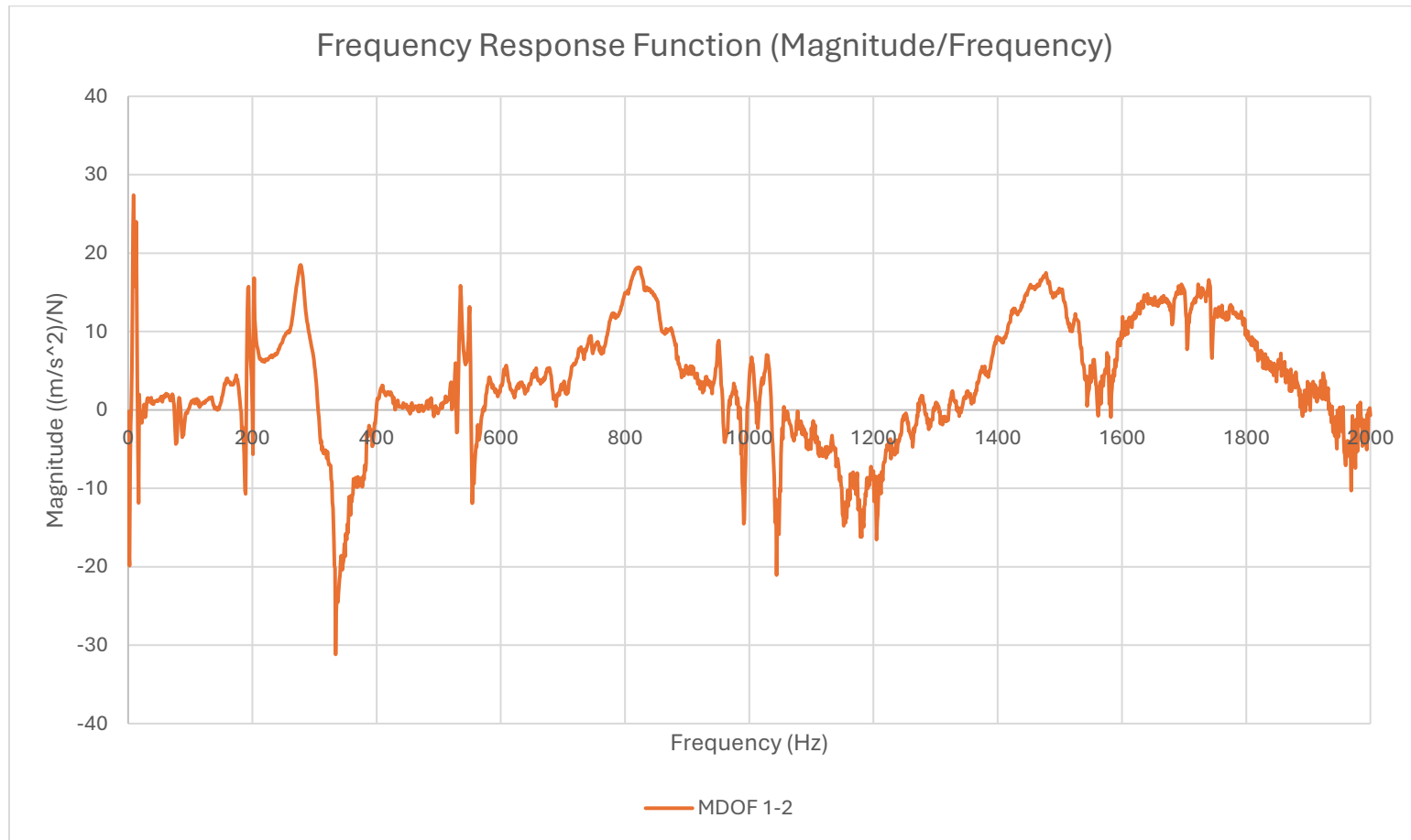
MDOF 1-1 Inverse (Real) FRF - Frequency 5



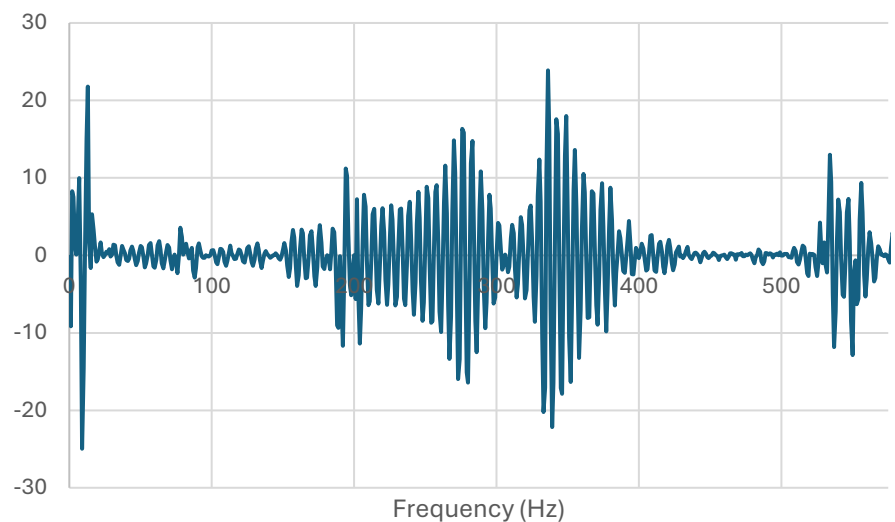
MDOF 1-1 Inverse (Img.) FRF - Frequency 5



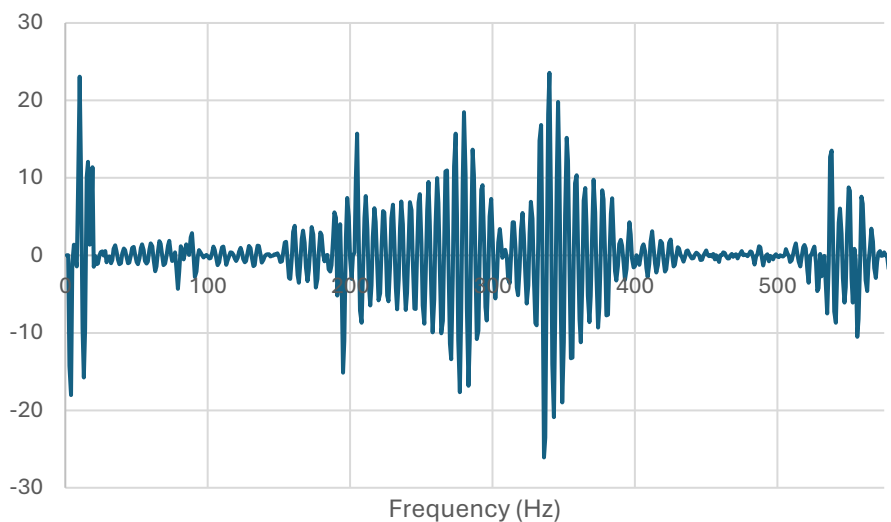
3. MDOF 1-2



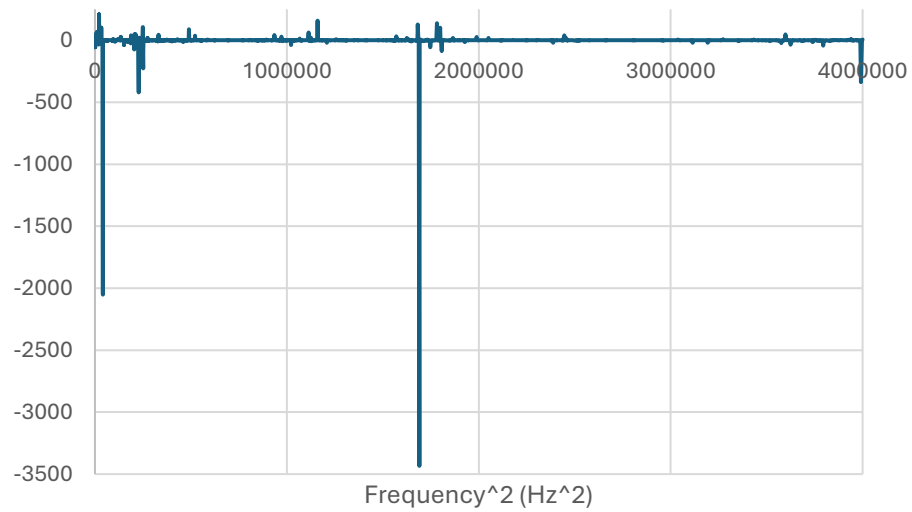
Real Component of the MDOF 1 - 2 FRF



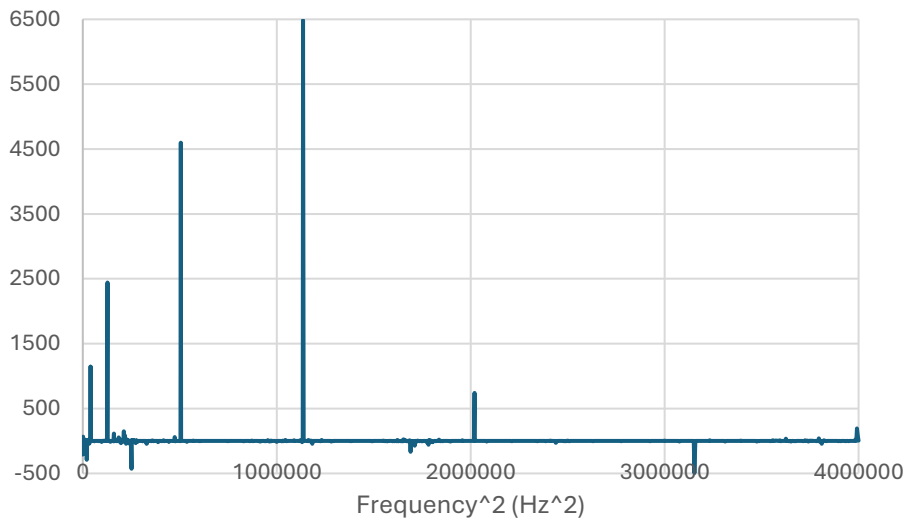
Imaginary Component of the MDOF 1 - 2 FRF



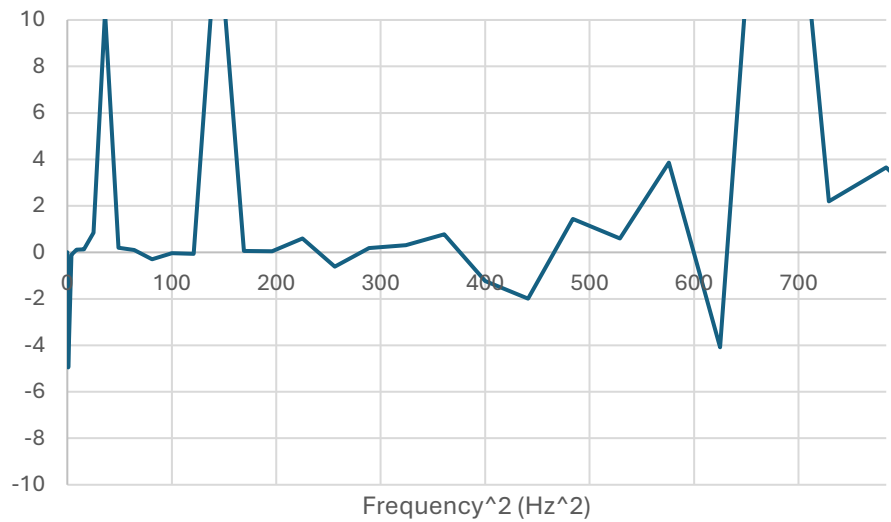
Inverse FRF (Real) MDOF 1-2



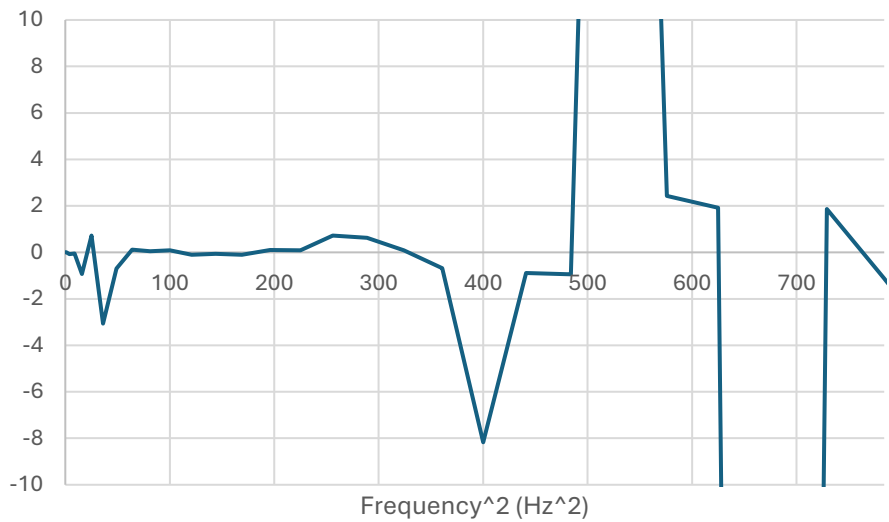
Inverse FRF (Imaginary) MDOF 1-2



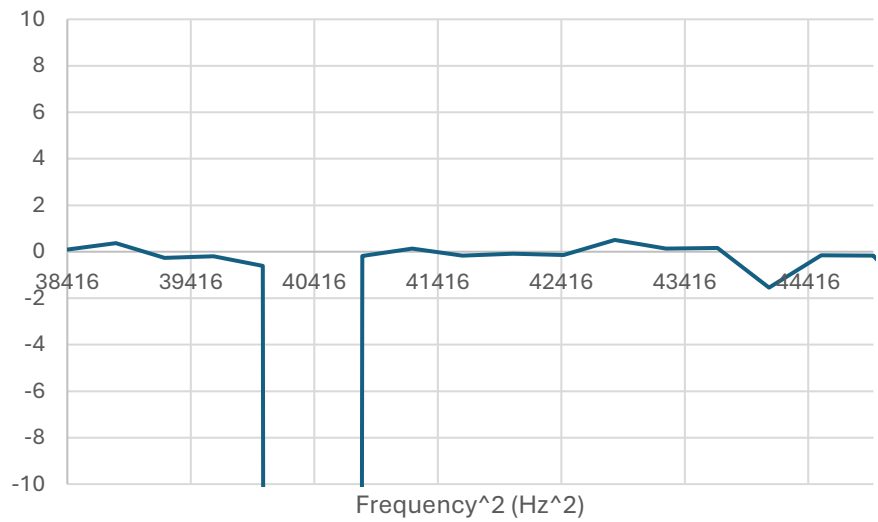
MDOF 1-2 Inverse (Real) FRF - Frequency 1



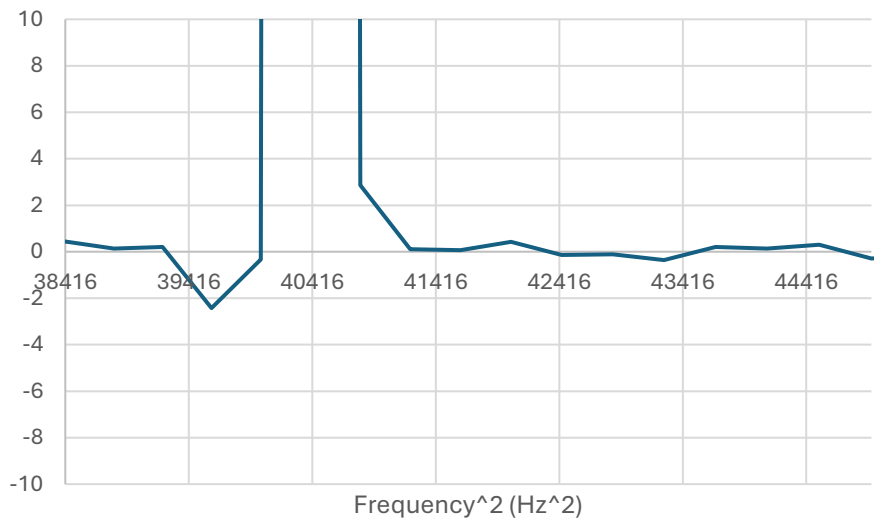
MDOF 1-2 Inverse (Img) FRF - Frequency 1



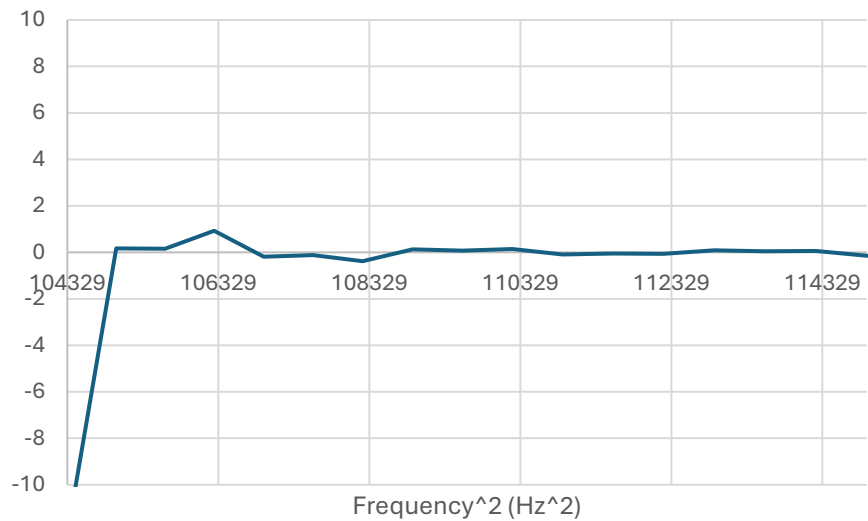
MDOF 1-2 Inverse (Real) FRF - Frequency 2



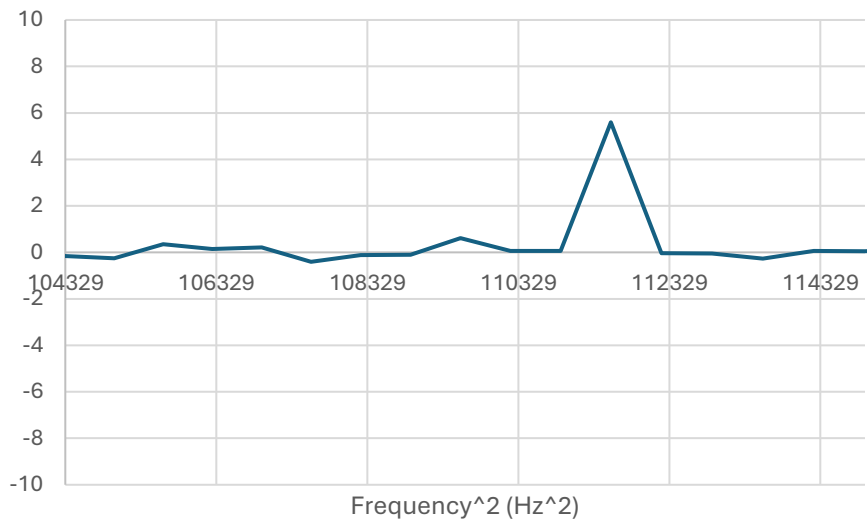
MDOF 1-2 Inverse (Img) FRF - Frequency 2



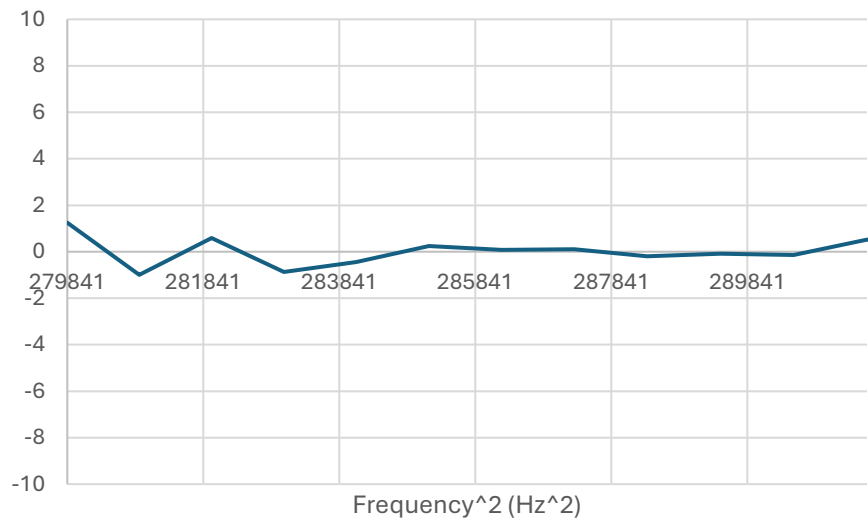
MDOF 1-2 Inverse (Real) FRF - Frequency 3



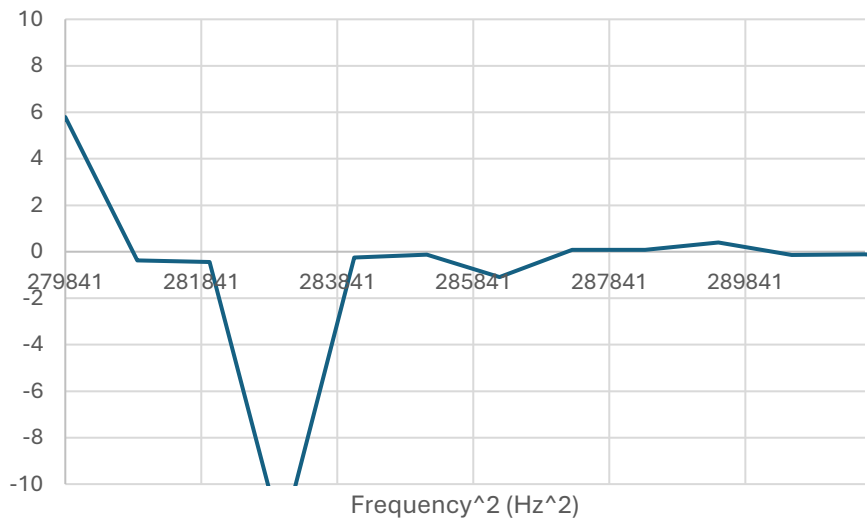
MDOF 1-2 Inverse (Img) FRF - Frequency 3



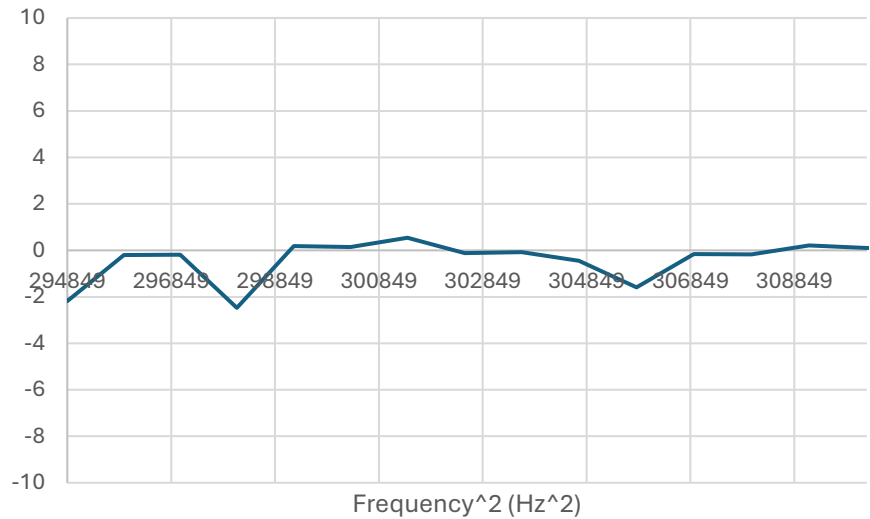
MDOF 1-2 Inverse (Real) FRF - Frequency 4



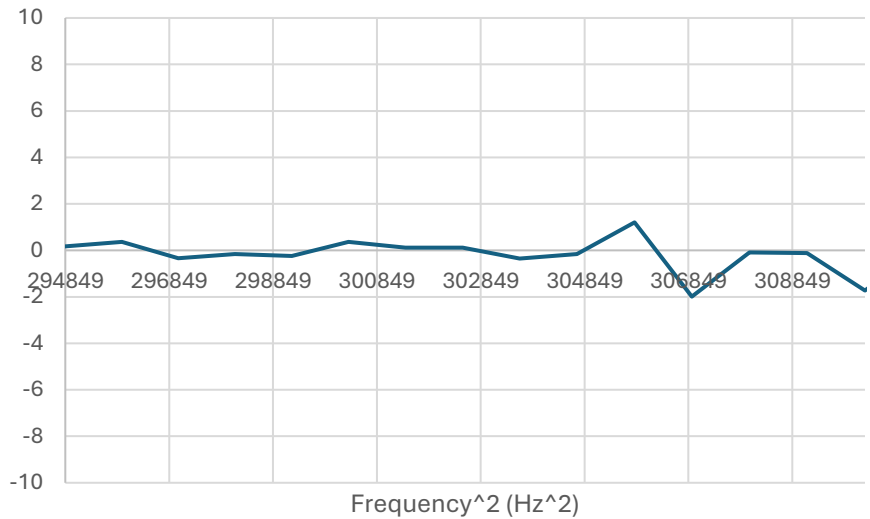
MDOF 1-2 Inverse (Img) FRF - Frequency 4



MDOF 1-2 Inverse (Real) FRF - Frequency 5



MDOF 1-2 Inverse (Img) FRF - Frequency 5



Appendix E – Author Contributions

Table 6 - Contributions of each author to the report by section.

Author	Contribution
Sofia Bertocci	Chapter 3: Modal Test & Analysis (Deriving final experimental frequencies)
Oriol Jo López	Chapter 2: Theoretical Description (Full chapter) Chapter 5: Conclusion (Full chapter)
Rowan Lawlor	Chapter 3: Modal Test & Analysis (Finding inverse lines-of-fit) Chapter 4: Discussion (Full chapter)